



Very high-resolution terrain surveys of the Chã das Caldeiras lava fields (Fogo Island, Cape Verde)

Gonçalo Vieira¹, Carla Mora¹, Pedro Pina², Ricardo Ramalho^{3,4,5,6}, Rui Fernandes⁷

¹Centre of Geographical Studies (CEG), IGOT, University of Lisbon, Lisbon, 1600-276 Lisboa, Portugal

5 ²Centre of Natural Resources and Environment (CERENA), IST, University of Lisbon, Lisbon, 1049-001 Lisboa, Portugal

³Instituto Dom Luiz (IDL), Faculdade de Ciências, Universidade de Lisboa, 1749-016 Lisboa, Portugal

⁴Departamento de Geologia, Faculdade de Ciências, Universidade de Lisboa, 1749-016 Lisboa, Portugal

⁵School of Earth Sciences, University of Bristol, Wills Memorial Building, Queen's Road, Bristol BS8 1RJ, UK

10 ⁶Lamont-Doherty Earth Observatory, Columbia University, Comer Geochemistry Building, PO Box 1000, Palisades, NY10964-8000, USA

⁷Instituto Dom Luiz (IDL), Universidade da Beira Interior, Covilhã, 6201-001 Covilhã, Portugal

Correspondence to: Gonçalo Vieira (vieira@igot.ulisboa.pt)

Abstract. Fogo in the Cape Verde archipelago off Western Africa is one of the most prominent and active ocean island volcanoes on Earth, posing an important hazard to both local populations and at a regional level. The last eruption took place
15 between 23 November 2014 and 8 February 2015 in the Chã das Caldeiras area at an elevation close to 1,800 m above sea level. The eruptive episode gave origin to extensive lava flows that almost fully destroyed the settlements of Bangaeira, Portela and Ilhéu de Losna. In December 2016 a survey of the Chã das Caldeiras area was conducted using a fixed-wing unmanned aerial vehicle and RTK GNSS, with the objective of improving the mapping accuracy derived from satellite
20 platforms. The main result is an ultra-high resolution 3D point cloud with a Root Mean Square Error of 0.08 m in X, 0.11 m in Y and 0.12 m in Z, which provides unprecedented accuracy. The survey covers an area of 23.9 km² and used 2909 calibrated images with an average ground sampling distance of 7.2 cm. A digital surface model and an orthomosaic with 25 cm resolution are provided, together with elevation contours with an equidistance of 50 cm and a 3D texture mesh for visualization purposes. The delineation of the 2014-15 lava flows shows an area of 4.53 km² by lava, which is smaller but more accurate than the previous estimates from 4.8 to 4.97 km². The difference in the calculated area, when compared to
25 previously reported values, is due to a more detailed mapping of flow geometry and the exclusion of the areas corresponding to kīpukas. Our study provides an ultra high-resolution dataset of the areas affected by Fogo's latest eruption – crucial for local planning – and provides a case study to determine the advantages of ultra high-resolution UAV surveys in disaster-prone areas. The dataset is available for download at <http://doi.org/10.5281/zenodo.4035038> (Vieira et al., 2020).

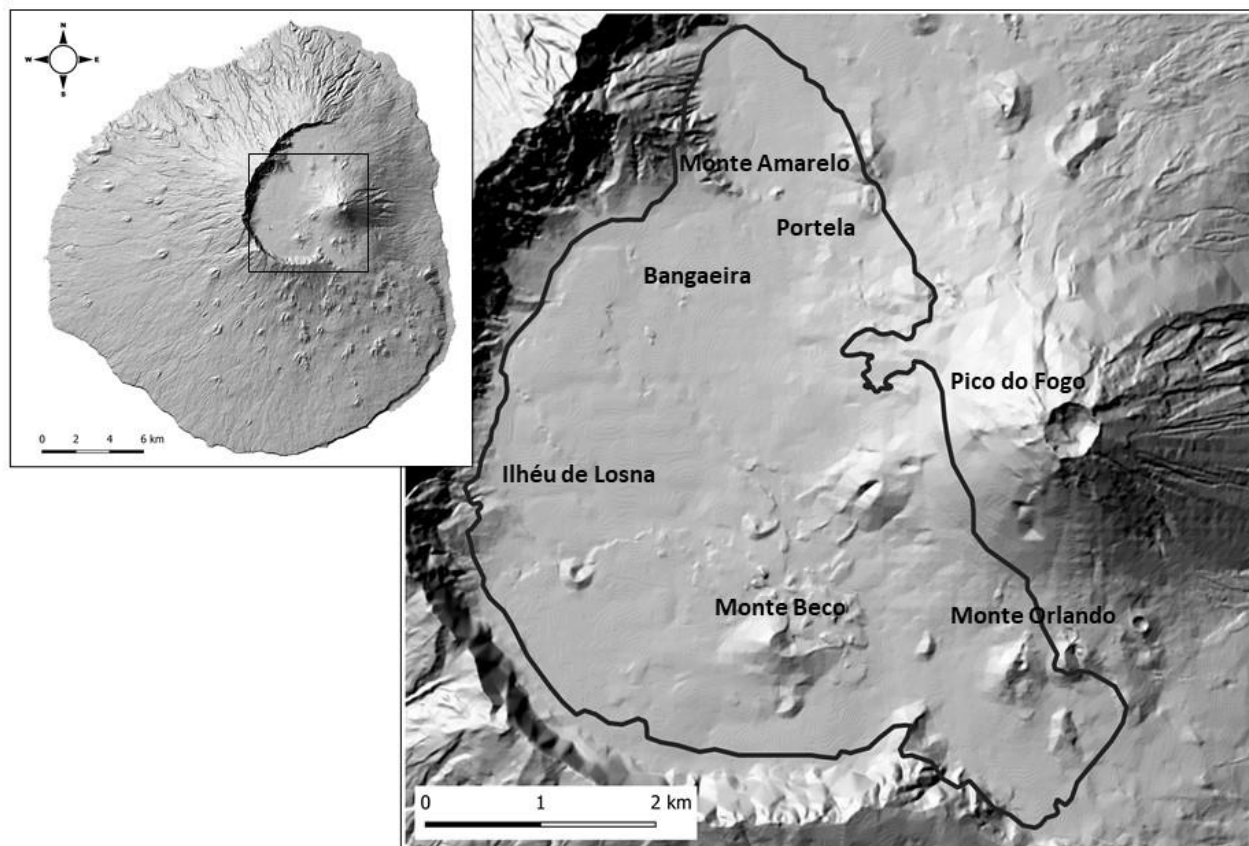
1. Introduction

30 Detailed knowledge on volcanic eruptions, their products, evolution and impacts is of paramount importance for volcanic hazard assessments and to advance our capability to forecast the likely behaviour of future eruptions. Volcanic eruptions may incur in considerable loss of life and lasting damage to infrastructures, particularly on Small Developing Island States



35 like Cape Verde, where volcanic eruptions are likely to have disproportionate impacts, on account of their more limited
resources and geographical isolation (Komorowski et al., 2016). Accordingly, solid and realistic volcanic hazard assessments
in such areas, more than in any other settings, greatly benefit from very-high resolution datasets from which detailed
volcanological, geophysical, and environmental parameters can be inferred. In particular, very high-resolution digital terrain
40 datasets of recently erupted lava-flow fields, may provide rapidly produced topographical datasets that can also be used to
plan mitigation and reconstruction strategies, as well as the opening of vital new communication infrastructures. The
usefulness of such datasets is greatly enhanced when these datasets are freely available to governmental agencies, decision-
45 making bodies and the scientific community alike. In line with this vision, in this paper we report and make available a
recently acquired very high-resolution digital surface model and orthomosaic of the lava flow-flow field created during the
2014-15 eruption of Fogo volcano in Cape Verde.

Fogo in the Cape Verde Archipelago off Western Africa is one of the most prominent and active ocean island volcanoes on
Earth, posing an important hazard to both local populations and at a regional level (Day et al., 1999; Heleno da Silva et al.,
45 1999; Ramalho et al., 2015; Eisele et al., 2015; Jenkins et al. 2017). Crucially, Fogo is the site of recurring volcanic activity,
with a record of at least 27 historical eruptions since the island was discovered in the mid-fifteenth century, yielding a mean
recurrence interval between eruptions of approximately 19.8 years, with individual intervals ranging from 1 to 94 years
(Ribeiro, 1954; Torres et al., 1998; Day et al., 1999; Mata et al., 2017). The latest events occurred in 1995 and in 2014-15,
50 both of which extruded extensive lava flow fields at the Chã das Caldeiras, a summit depression lying at an elevation of
approximately 1800 m above mean sea level. Effectively, the settlements of Bangaeira, Portela and Ilhéu de Losna located in
Chã das Caldeiras were almost fully destroyed in the 2014-15 eruption (Fig. 1). With a population of about 1200 inhabitants
prior to the eruption, the local economy was based in agriculture (mainly wine and fruit orchards), grazing, and tourism.
Fortunately, there were no casualties.



55 **Figure 1 – Location of the Chã das Caldeiras and of the surveyed area (black line) in Fogo Island (Cape Verde). Shaded relief derived from the DEMFI (2010) 5 m DEM.**

The latest eruption started on the 23rd November 2014 and lasted until the 8th February 2015, with magma being erupted from a 700 m-long NE–SW trending eruptive fissure located on the SE flank of the previous 1995 crater row, on the SW flank of Pico do Fogo (Vieira et al., 2016; Mata et al., 2017). Reportedly, the eruption started with vigorous fire-fountain activity, which quickly evolved to a more explosive strombolian style, forming a crater row roughly parallel to the 1995
60 fissure. Later, the eruption was characterized by simultaneous or alternating hawaiian, strombolian and vulcanian eruptive styles (from the different craters of the fissure) lasting for several days, and by an almost constant emission of lava flows from the lowermost terminus of the vent (Mata et al., 2017). These formed two initial thick ‘a’ā flow lobes: the first advanced towards the southwest and eventually stalled after 1.7 km, at the foot of the caldera wall; the second progressed
65 intermittently 3 km to the northeast, towards the village of Portela, razing a large portion of this settlement (Mata et al. 2017; Jenkins et al., 2017). During the later stages of the eruption, however, this flow lobe was reactivated, producing more fluid



‘a’ā and pāhoehoe breakouts to the west and north, the latter of which destroyed most of what was left of the Portela settlement and descended to the village of Bangaeira, causing widespread destruction there (Mata et al. 2017; Jenkins et al., 2017). The resulting lava flow field affected an area of ci. 4.8 km², with extruded volumes estimated at $\sim 45 \times 10^6$ m³ (Bagnardi et al., 2016; Richter et al., 2016; Cappello et al. 2016).

Remote sensing techniques have been used by several authors to study the Fogo eruption of 2014-15. Capello et al. (2016) used the HOTSAT satellite thermal monitoring system for the analysis of MODIS and SEVIRI data for the location of the hotspot, lava thermal flux, and effusion rate estimation. To forecast lava flow hazards during the 2014-15 Fogo eruption they used the MAGFLOW model. Validation of numerical simulations was done using Landsat 8 OLI and EO-1 ALI images and field observations. Bagnardi et al. (2016) used very high-resolution tri-stereo optical imagery acquired by the Pleiades-1 satellite constellation and generated a 1 m resolution digital elevation model (DEM) of the Fogo Volcano. From the Pleiades-1 post-eruption topography they subtracted the heights from a pre-eruption DEM, that was obtained using spaceborne synthetic aperture radar (SAR) data from the TanDEM-X mission. To measure the subsidence of the lava flow field, they used Sentinel-1 for interferometry. Height differences between the post-eruptive Pleiades-1 DEM and the pre-eruptive topography from TanDEM-X show a lava volume of $45.83 \pm 0.02 \times 10^6$ m³, emplaced over an area of 4.8 km² at a mean rate of 6.8 m³/s. Richter et al. (2016) did lava flow simulations based on field topographic mapping and satellite remote sensing analysis. They produced a topographic model of the 2014-15 lava flows from combined Terrestrial Laser Scanner (TLS) and photogrammetric data. The pre-eruptive DEM used was 5 m/pixel and was generated from the contours based on photogrammetric data. They estimated a lava flow volume of $43.7 \pm 5.2 \times 10^6$ m³. TerraSAR-X imagery was used to access the lava flow model performance. The authors point out the need of having up-to-date topographic information because lava flow hazards change as result of topography modifications.

More recent, Bignami et al. (2020) used a combined method of 21 images from Sentinel-1, COSMO-SkyMed, Landsat 8, and Earth-Observing-1 missions from November 2014 to January 2015, to retrieve lava flow patterns. They applied an automatic change detection technique for estimating the lava field and its temporal evolution, combining the SAR intensity and the interferometric SAR coherence. Results showed a SW-NE oriented dyke, located inside Chã das Caldeiras, SW of the Pico do Fogo, as reported by Gonzalez et al. (2015). The area coverage of the lava flow obtained by visual analysis (L8 and EO-1) was estimated at 4.97 km² as in Cappello et al. (2016), very close to the 4.8 km² estimated by Bagnardi et al. (2016), and the 4.85 km² estimated using Terrestrial Laser Scanner (TLS) combined with structure from motion data by Richter et al. (2016).

Several papers have been published on the latest eruption of the Fogo volcano, e.g. focusing on the variation of land surface temperatures during the eruption (Vieira et al., 2016), on lava geochemistry and small-scale mantle heterogeneity (Mata et al., 2017), mineralogy and geochemistry of incrustations (Silva et al., 2019), conduit dynamics and surface deformation (Gonzalez et al. 2015), on lava flow mapping and volume estimates (Bagnardi et al. 2016; Bignami et al., 2020), and lava flow hazards (Richter et al., 2016; Cappello et al. 2016; Jenkins et al., 2017).



100 In the remit of the project FIRE (Fogo Island volcano: multidisciplinary Research on 2014/15 Eruption, funded by FCT-
Portugal), an extensive survey using a survey-grade unmanned aerial vehicle (UAV) was conducted in December 2016 with
the purpose of generating a very high resolution digital elevation model (DEM) and orthomosaic of the lava field to be used
as baseline data for assessment of the eruption impacts, support to geological mapping and studies of the lava flow field, as
well as for modelling lava flow dynamics. A study commissioned by the United Nations Development Program in Cape
105 Verde stresses that an improvement in the assessment of hazards on the island of Fogo can only be achieved from a detailed
analysis and the modelling of the lava flow (Fonseca et al., 2014). The data presented here is the result of that campaign and
is the most detailed and updated survey of the area, with an ultra-high resolution digital surface model (DSM) that is
essentially a DEM in most of the area due to the overall lack of vegetation and scarce number of buildings, and a digital
orthomosaic.

110 2. Application of UAVs to volcanic areas

Digital elevation models and the dissemination of Geographical Information Systems have changed the way the terrain is
characterized, analysed, monitored and modelled, especially since the 1990's. DEMs have been produced from dense
collections of topographical points, manned aircraft photogrammetry, digitizing of topographic maps (Stevens et al., 1999),
satellite remote sensing (Baldi et al., 2002; Kerle, 2002; Diefenbach et al., 2013), light detection and ranging - LiDAR
115 (Mouginis-Mark and Garbeil, 2005; Mazzarini et al., 2007; Favalli et al., 2009; Fornaciai et al., 2010), radar interferometry
(InSAR) (Rowland et al., 1999; Poland, 2014). Since the mid-2010's, with the technological developments and decreasing
cost of unmanned aerial vehicles, accompanied by the development of photogrammetry software and computing power, a
revolution took place. Very accurate and high quality DEMs became increasingly available, leading to the possibility to easily
achieve centimetric to decimetric resolution, even in large areas. The number of UAV-based surveys have been increasing
120 steadily but many of them stay stored in the producers or client computers and are not of open-access.

UAVs have had various applications, such as for wildlife recognition (e.g. Christiansen et al., 2014; Wang et al., 2019),
agriculture (e.g. Hassan-Esfahani et al., 2015, Kattenborn et al. 2014; Hasseler and Baysal-Gurel, 2019), urban and civil
engineering (Westfeld et al., 2015), archaeology (Campana 2017; Risbøl and Gustavsen 2018), coastal dynamics
(Chikhradze et al 2015; Brunier et al 2016; Turner et al 2017; Long et al 2016), climatology (Lindgren et al 2015; Bühler et
125 al 2016), geomorphology (Lucieer, et al 2014; Dabski et al. 2020), vegetation in Polar regions (Mora et al 2015, Miranda et
al 2020), glacier monitoring (Benoit et al 2019; Jouvét et al 2020) or for monitoring volcanic systems (Chio and Lin, 2017;
Thiele et al., 2017).

Applications of UAV surveys to research in the Earth and Atmosphere sciences are relatively recent, having begun to
emerge with greater expression from 2014 (Colomina and Molina 2014; Pajares 2015). Since then the number of
130 publications has grown rapidly and spread across research fields, developing into a technique allowing fast and low-cost
access to high spatial resolution data (Gomez and Purdie, 2016). The high versatility and possibilities of surveying even



rough terrains of difficult access, such as the situation of volcanic eruptions, make UAVs a powerful tool to acquire real-time or near-real-time data on processes that often cannot be observed by naked eye (Di Felice et al 2018). Hence UAVs are increasingly used in situations of risk where it is essential to make the rapid terrain recognition following natural disasters (Gomez and Purdie 2016). Software and computing power have evolved very fast in last decade and the application of advanced photogrammetry algorithms involving image matching and structure from motion started to allow facilitated production of high-quality digital surface models and orthophoto maps. The collection of accurate GNSS ground control points allows to generate these products with centimetre resolution and accuracy (Favalli et al 2018). The recent development of RTK UAVs allows for even faster workflows in the terrain and to produce highly accurate models.

140 Photogrammetry techniques have been widely applied to study detailed changes in the morphology and structures of volcanos, like Mount St. Helens, the Colima and the Merapi (Major et al., 2009; Walter et al., 2013; Salzer et al., 2016). Optical and thermal cameras transported on UAVs have been used for identifying meter to sub-meter topography changes and for the detection of thermal anomalies (Nakano et al., 2014; Thiele et al., 2017; Nakano et al., 2014; Müller et al., 2017; Amici et al., 2013; Di Felice et al 2018). In addition, specific payload sensors are being used for measuring volcanic gas fluxes (McGonigle et al., 2008; Liu et al. 2019; de Moor et al., 2019), gas sampling (Mori et al., 2016; Rüdiger et al., 2018; Stix et al., 2018) and sediment sampling (Yajima et al., 2014).

Various studies have shown the potential of UAV-based surveying in volcanic terrains. These show the potential of the survey produced at Fogo, not only for characterizing post-eruption changes, but also for providing baseline data for analysing the dynamics of the lava flow fields upon cooling, or the soil erosion and even human reoccupation of the area. As examples of UAV-based mapping, at the Nishinoshima Volcano, Nakano et al (2014) have acquired visible imagery to produce 3D maps allowing to monitor the evolution of the volcano. Darmawan et al. (2018) studied morphological and structural changes from 2012 to 2015 at the Merapi lava dome having identified the locations of steam-driven explosions. Felice et al. (2018) surveyed the erupting crater of Indonesian Lusi mud eruption as it was spewing boiling mud, water, aqueous vapour, CO₂, CH₄. Favalli et al. (2018) generated a high spatial resolution digital terrain model and orthomosaic of Mount Etna's January–February 1974 lava flow field, allowing the analysis of the morphology of sub-meter features, such as folds, blocks, and cracks, over kilometre-scale areas. The 3-cm orthomosaic allowed the analysis of centimetre-scale grain size distribution of the lava surface. Müller et al. (2017) studied the 2014–15 fissure eruptions of the Holuhraun to investigate the link between magma dikes at depth and the association with elastic and inelastic surface deformation. Turner et al (2017) during the 2014–15 Pāhoehoe crisis, used a UAV to monitor the front of a slowly advancing pāhoehoe lava flow. UAV surveys allowed Bonali et al. (2019) to study volcano-tectonics and tectonic features in an active Icelandic rift with unprecedented detail in extended areas in a much faster way and much lesser funds with respect to traditional field activity. One of the first UAV surveys during an ongoing eruption was performed by De Beni et al. (2019) in the 27 February–02 March 2017 event of Mt. Etna, which allowed improving the monitoring quality of the lava flow in terms of timeliness and detail. The independent acquisition of both visible and thermal infrared imagery by a pair of UAV in Stromboli allowed Wakeford et al. (2019) to build a 3D photogrammetric model of an active volcano. Finally, a recent summary about the use of small UAV



for collecting immediate and real-time aerial data in volcanic environments during and after an eruption is provided by Jordan (2019), highlighting its advantages for mapping, sample collection, thermal imaging, magnetic surveys, slope stability studies, and also as platforms for carrying outgassing measurement sensors.

3. The study area and the volcanic activity of 2014-15

- 170 The island of Fogo is one of ten islands of Cape Verde, an archipelago located off the west African coast, about 600 km from Senegal. The Cape Verdes are regarded as the type-example of a volcanic archipelago formed in a stationary plate environment relatively to its hotspot, which probably explains the arcuate distribution of its islands (Burke & Wilson 1972; Lodge and Helffrich, 2006; Ramalho et al., 2010a, 2010b, 2010c; Ramalho, 2011). In more detail, this arcuate geometry is defined by two island chains: a “northern”, from São Nicolau to Santo Antão, and a “eastern-to-southern”, from Sal to
- 175 Brava. There is no evident hotspot track but there is a morphological suggestion of an age progression in the “eastern-to-southern chain”, from east (oldest islands) to west (youngest islands), which is supported by ages of the oldest exposed lithologies (see Ramalho, 2011). Fogo is located close to the southern terminus of this latter chain and is the only island in the archipelago with historical (i.e. last 500 years) eruptions (Bebiano, 1932; Ribeiro, 1954; Machado, 1965; Day et al., 1999; Faria and Fonseca, 2014).
- 180 Fogo is a large ocean island volcano showing a conical shape with a diameter of about 30 km (at sea level) and rising to an elevation of 2829 m, approximately 7 km above the surrounding seafloor. Structurally, the island is a compound volcano, featuring a “somma-vesuvio” association, with a younger stratovolcano – Pico do Fogo – rising from the central depression – Chã das Caldeiras – of an older collapsed volcano, sometimes referred as Monte Amarelo (Ribeiro, 1954; Day et al., 1999). This depression, however, is open to the east, being limited in the remaining three sides by a horseshoe shaped steep rock
- 185 wall, over 1,000 m high, called Bordeira. This morphology, in turn, is either interpreted as a gravitational collapse headwall (Day et al., 1999; Paris et al., 2011) or as volcanic caldera walls, whose eastern portion later experienced a gravitational flank failure (Torres et al., 1998; Brum da Silveira et al., 1997a, 1997b; Madeira et al., 2008). Notwithstanding the different interpretations for the origins of this summit depression, it is clear that the opening to the east resulted from a massive flank failure of the flank of the volcano. Effectively, marine geophysical surveys undertaken off Fogo revealed the presence of
- 190 voluminous submarine debris avalanche deposits extending offshore into the channel between Fogo and Santiago, and into the seafloor south and north of these islands, thus attesting the occurrence of this collapse (Le Bas et al., 2007; Masson et al., 2008; Barrett et al., 2019b). Moreover, field evidence attesting to the impact of a megatsunami triggered by Fogo’s flank failure has been documented in the neighbouring islands of Santiago (Paris et al., 2011, 2018; Ramalho et al., 2015) and Maio (Madeira et al., 2020), confirming the catastrophic nature of the collapse and suggesting a 65-84 ka age for this event.
- 195 Pico do Fogo, currently the highest point in the island (2829 m in elevation), is a large and roughly symmetrical strato-cone that grew on top of the collapse scar, partially infilling this feature (Ribeiro, 1954; Torres et al., 1997; Brum da Silveira et al., 1997a, 1997b; Day et al., 1999). The sheer volume of this volcanic edifice is a testimony to the vigorous eruptive activity



taking place at Fogo Island. There have been suggestions that Pico do Fogo experienced summit eruptions as late as the 18th century (Day et al., 1999), however this seems to be contradicted by the stratigraphic sequence at the summit, which exhibits mostly altered volcanic successions. Effectively, historical records suggest that all historic eruptions were extruded from adventitious vents localised at the base and lower flanks of Pico do Fogo, or at Chã das Caldeiras and the eastern flank of the island, in the periphery of this strato-cone (Ribeiro, 1954; Torres et al., 1997; Brum da Silveira et al., 1997a, 1997b). This is the case of the 1951, 1995, and 2014-15 eruptions, which vents were located in the NW, SW and S flanks of Pico do Fogo, close to its base at Chã das Caldeiras.

Chã das Caldeiras (Fig. 2) is thus a lava-infilled high-altitude summit depression, which resulted from the gradual accumulation and ponding of lava flows (and pyroclasts) erupted from Pico do Fogo and its adventitious/satellite cones, against the vertical walls of Bordeira. Morphologically, Chã can be divided in two large semi-circular sectors: a southern, larger, with approximately 3 km of radius, and with an elevation of 1780 m, and a northern, with a shorter radius of approximately 1 km, and with a mean elevation of 1650 m. These two sectors, which are roughly separated by the prominent Monte Amarelo spur, have been interpreted as two coalescent volcanic calderas by Torres et al. (1997), Brum da Silveira et al. (1997a, 1997b), and Madeira et al. (2008). Chã das Caldeiras is a generally flat landscape, punctuated by a few volcanic cones and extensively covered by ‘a‘ā and pāhoehoe lava flows and ash and lapilli deposits, which make it very irregular in detail and a challenging terrain for mapping. In particular, the extensive ‘a‘ā lava flow lobes of the 2014-15, 1995 and 1951 eruptions covered large portions of Chã, resulting in large swaths of virtually inaccessible rocky surfaces, given their extreme roughness. Hummocky landscapes also exist, generally corresponding to older ‘a‘ā lava flow fields with scattered large rafted blocks of spatter sequences in its surface (resulting from the gravitational collapse of strombolian cones and subsequent transport by lava flows), which are now partially buried under a blanket of lapilli and ash that smoothed the surface. A good example of such surfaces can be found to the east and particular to the west of the Monte Beco cone, being genetically associated to this vent. The foot and slopes of Pico do Fogo, in contrast, are extensively covered by a thick blanket of lapilli and ash, conferring a very smooth and uniform conical surface. Despite this cover, fanned leveed channelled morphologies can also be recognized at the foot of Pico do Fogo, corresponding to buried lava flow fans and alluvial fans. Overall, vegetation is scarce and is mostly confined to the surfaces of talus accumulated at the foot of Bordeira, where a thin soil exists, or to some scattered vineyards along some ash-covered slopes.



225

Figure 2 – The Chã das Caldeiras and Pico do Fogo during the 2014-15 eruption. View towards the southeast with the ‘a’ā lava flows of 2014-15 in the foreground.

Human settlement at Chã das Caldeiras started towards the end of the 19th century (Ribeiro, 1954). Chã, as a high-altitude
230 depression, is cooler and more humid than the rest of the island, with frequent fog condensation and occasional frosts,
providing ideal conditions for the planting of orchards and vineyards. Attracted by the prospect of a more prosperous
agriculture, people gradually settled Chã, mostly in the vicinities of Monte Amarelo, where some water springs and
enhanced but ephemeral flow (from the larger canyons draining Bordeira) allowed easier access to water. Here they
established the settlements of Portela, Boca Fonte, and later Bangaeira, which slowly and gradually grew in size until the
235 1995 eruption, when Boca Fonte was all but destroyed and the main access road to these settlements was blocked by the
advancing flows (the 1951 eruption, although of a higher magnitude, had a lower impact in these settlements; Jenkins et al.,
2016). After the 1995 eruption, however, the prospect of an additional income provided by a burgeoning wine industry and
the rapidly growing flow of tourists that came to see the volcano, fuelled the rapid growth of Portela and Bangaeira, with
population reaching as much as ~1500 resident inhabitants by 2014 (Fonseca et al., 2014; Jenkins et al., 2016). The
240 2014/2015 eruption, in contrast, had a profound impact in these villages, given that the advancing lava flows either razed or



buried up to 90% of the existing buildings, as well as covered large swaths of the adjacent agricultural land. Gradually, however, reconstruction is taking place, either through new constructions over the recent lava flows, or by the painstaking reclamation of lava-buried but structurally intact buildings.

3. Methods

245 3.1 UAV Surveying

The field campaign was conducted about 20 months after the end of the eruption of 2014-15, when the lava flows had already cooled substantially, but with the occupation of the few houses existing at the Chã das Caldeiras, being forbidden and still hazardous, mainly due to gas emissions. Hence, the field team stayed at the village of São Filipe and travelled daily to the survey area. The expertise of the team on local conditions, geology and logistics and cooperation with the Cape Verde
250 authorities, greatly facilitated the success of the mission.

The main challenges to overcome were i. the weather, which in December frequently shows high winds and low visibility (clouds) in the Chã das Caldeiras, ii. finding good landing sites for the UAV, iii. coping with the 1000 m high vertical rock wall of the Bordeira and with its possible influence on the positioning and communications system of the UAV, and iv. collecting enough high-quality ground control points.

255 The survey of the Chã das Caldeiras area was conducted from 12 to 16 December 2016 with a field team of 4 members. Two members focussed on conducting the UAV flights and the other two on the collecting ground control points. Communications among team members were done using VHF radios.

The weather during the campaign was excellent with clear skies and no wind in the first days, but deteriorated towards the end of the week, with clouds entering the survey area and affecting initially the illumination conditions and even limiting the
260 flights in the last two days. This has affected the quality of the orthomosaic, which shows illumination artefacts in the northern part of the Chã das Caldeiras.

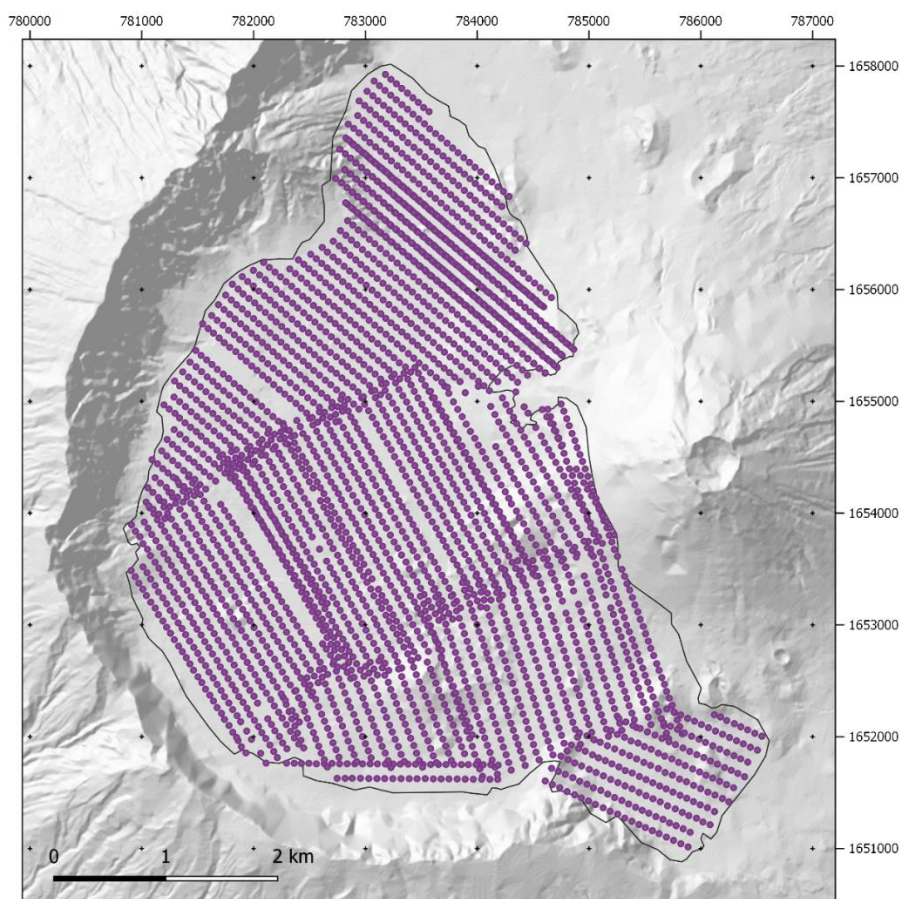
The survey was conducted using a professional survey-grade fixed-wing UAV SenseFly eBee classic, which has a structure of expanded polypropylene (EPP) foam, with carbon and composite parts. It has a 96 cm wingspan and under 0.7 kg take-off weight, which when disassembled allows for lightweight packing. This model allows for flights with wind speeds up to 45
265 km/h, flight durations of up to 50 min and a radio link distance up to 3 km. Two cameras were used: a Canon G9X 16MP in the initial flights, which had a critical failure, and a backup Canon IXUS 12 MP which was used subsequently.

Take-off with the eBee is performed by hand, which facilitates selecting the location, but landing is done normally in fully automatic mode needing several tens of meters of approach area, and a smooth landing surface in order not to damage the EPP UAV body. This was a significant limitation to the survey, since the area of the Chã das Caldeiras is mostly covered by
270 very rough lava surfaces, with scarce smooth ash and lapilli cover sites, which are normally far apart. Given these constraints, five sites allowing for good landing conditions were selected: (i) 14.93477° N, 24.35407° W, (ii) 14.928092° N,



24.353165° W, (iii) 14.92339° N, 24.356605° W, (iv) 14.9334999° N, 24.3722831° W and, (v) 14.962204° N, 24.3690256° W.

275 The survey consisted of 20 flights that do not show the ideal spatial setup nor homogenous illumination conditions in the resulting aerial photos, but it was the best solution given the logistical constraints. This was due to the following problems: sparse location of the take-off and landing sites, changes in wind-speed affecting power consumption, unexpected cloud advection and low visibility during some days, duration of daylight, fast changing shadowing effect from the Bordeira rock wall and by Pico do Fogo, battery limitations (due to heat, high risk of damaging the UAV in case of a need to crash land over lava flow, we decided not to conduct flight of over 30 min), long-distances to move between landing sites, these
280 resulting on the need for constant on-site modifications of the original flight planning. The average flight elevation above the ground was 190 m, resulting on an average ground sampling distance of 6 cm, over 2,900 aerial photos and a total surveyed area of 24 km² (Fig. 3).

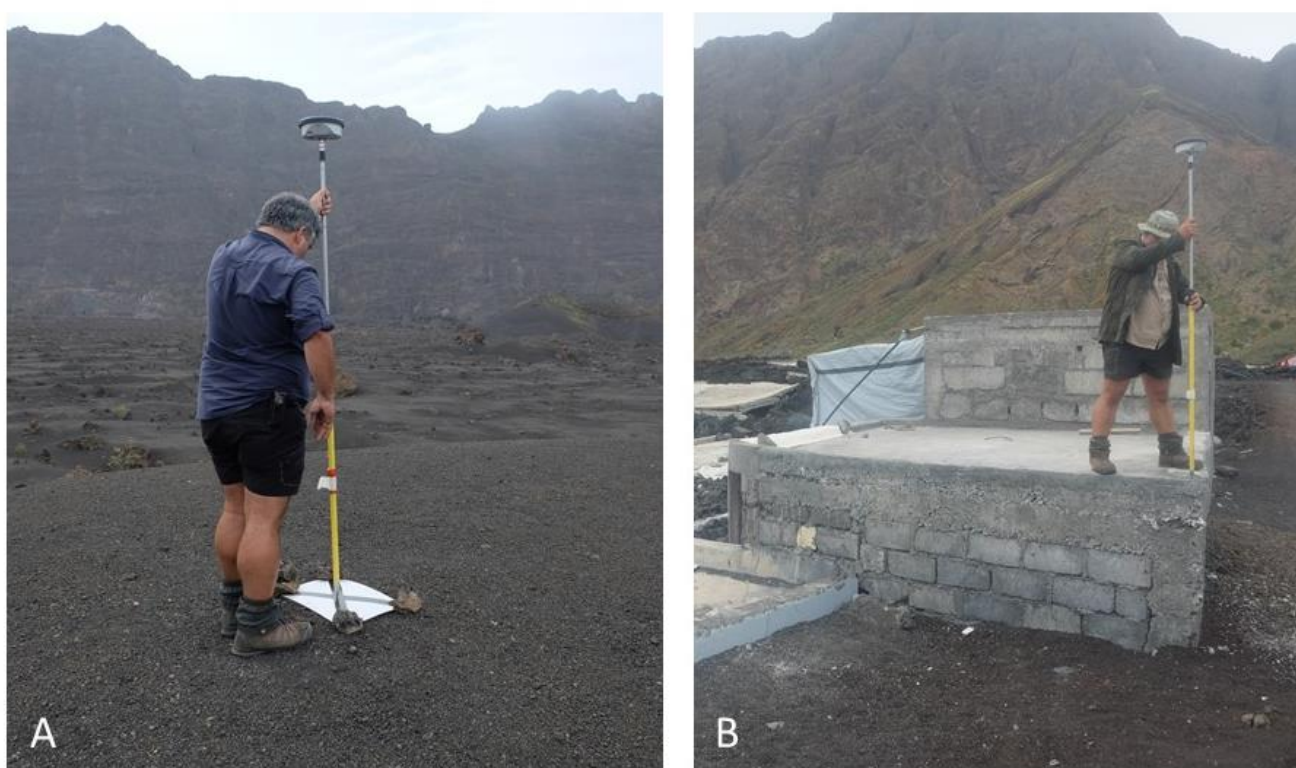


285 **Figure 3 – Aerial survey of the Chã das Caldeiras with the geolocation of the photographs, Shaded relief derived from the DEMFI (2010) 5 m DEM.**



3.2 Ground control points

Coordinates of ground control points (GCPs) were measured at markers distributed in the field prior to the survey and at easy identifiable points, such as large boulders and building edges. The measurements were obtained using a Leica Viva (GS08) GNSS with base stations located at known coordinate sites (Monte Beco and Monte Amarelo) and a rover for surveying in
290 RTK mode during the field surveys in December 2018. Extra GCPs were collected in February 2017 in small boulders selected in the preliminary orthophoto mosaic, in order to improve georeferencing quality. The accuracy of the GCP coordinates is of about 3 cm.



295 **Figure 4 – Ground control point collection with RTK GNSS. A. Using markers, B. Using existing points.**

3.3 Point cloud, orthophoto mosaic and digital surface model

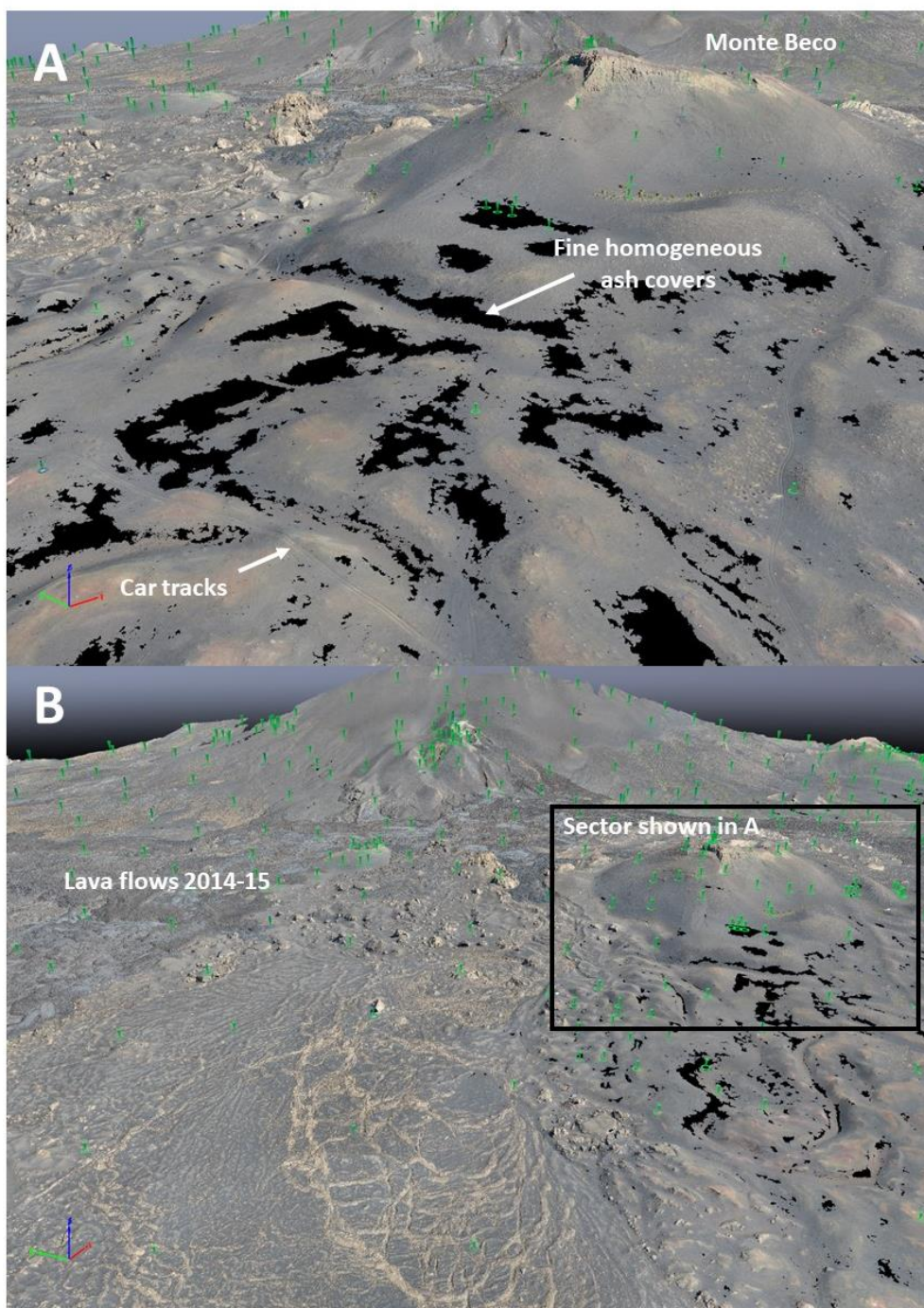
Aerial image processing was done using Pix4Dmapper 4.5.6, a commercial software based on automatic feature detection, image matching and modelling using structure from motion (SfM) algorithms. This process developed in the
300 1990s, results from the application of algorithms by automatic feature-matching. The SfM operates according to the basic



principles of stereoscopic photogrammetry, in which a 3D structure results from a series of 2D image overlays taken in motion to an object. The geometry of the images, position and orientation of the camera are calculated automatically without the need for a priori indication. Decisions are made simultaneously based on an iterative adjustment of package images, and the structures are automatically extracted from several overlapping images and the points are searched from image to image
305 allowing the estimation of the coordinates of the objects. The 3D point clouds are generated in an image-space coordinate system and are transformed into an absolute real-world object-space coordinate system. The transformation is achieved by using 3D functions based on a relatively small number of GCPs (Westoby et al. 2012; Smith et al. 2016).

The models that we have developed have used 2909 calibrated images with an average ground sampling distance of 7.17 cm and a total area covered of 23.89 km². The camera optimization resulted in a 0.35% difference between the initial and
310 optimized internal camera parameters. The images showed a median of 49521 key points per image and a median of 22632 matches per calibrated image. The large number of flights, large area and different illumination conditions led us to do separate processing and georeferencing of flights, with iterative project merging until the final model was obtained. In this process, we have used a total of 37 3D and 3 2D GCPs measured in the terrain. In order to improve the matching, 696 manual tie points were included, especially in areas covered by pyroclasts (lapilli and ash).

315 The point cloud was processed using full image scale, matching of image pairs using the aerial grid/corridor model and geometrically verified matching using automatic advanced key points extraction. The advanced camera calibration was done using the alternative method, internal parameters optimization (all), external parameters optimization (all) and no automatic rematch. The point cloud densification was done using multiscale and half-image size, with an optimal point density and a minimum number of 3 matches. This option was selected after intensive testing with 4 and 5 matches, which generated large
320 gaps in the point clouds, in areas which were well-resolved with 3 matches. The point cloud still shows sectors with no data in homogeneous fine ash and lapilli covers, but those areas are small as discussed below and always outside the recent lava fields (Fig. 5). Since the target of the 3D survey are the lava fields, we guarantee that those sectors are well represented with many accurate points in the cloud.



325

Figure 5 – Examples of areas without data in the 3D dense point cloud. **A.** Low quality areas in ash surfaces close to Monte Beco (car tracks pointed for scale), **B.** Most of the survey is of very high quality, with the figure showing the lava fields close to Monte Beco and the small areas with low quality. The green pins are manual tie points.



330 The final digital surface model (DSM) and orthomosaic are presented with a resolution of 25 cm/pixel, which allow for maintaining the root mean square error (RMSE) well below pixel size. Noise filtering and sharp surface smoothing were applied for the DSM, with interpolation using inverse distance weighting.

4. Modelling results and discussion

4.1 Point cloud

335 The point cloud model shows a RMSE of 0.08 m in X, 0.11 m in Y and 0.12 m in Z, evaluated using 13 independent check points (Table 1). Even after including several hundreds of manual tie points, it was not possible to obtain a good quality point cloud all over the survey area. Areas of homogeneous ash and pyroclasts covers lack 3D data, but they do not impact the overall mapping of the area, as is discussed below.

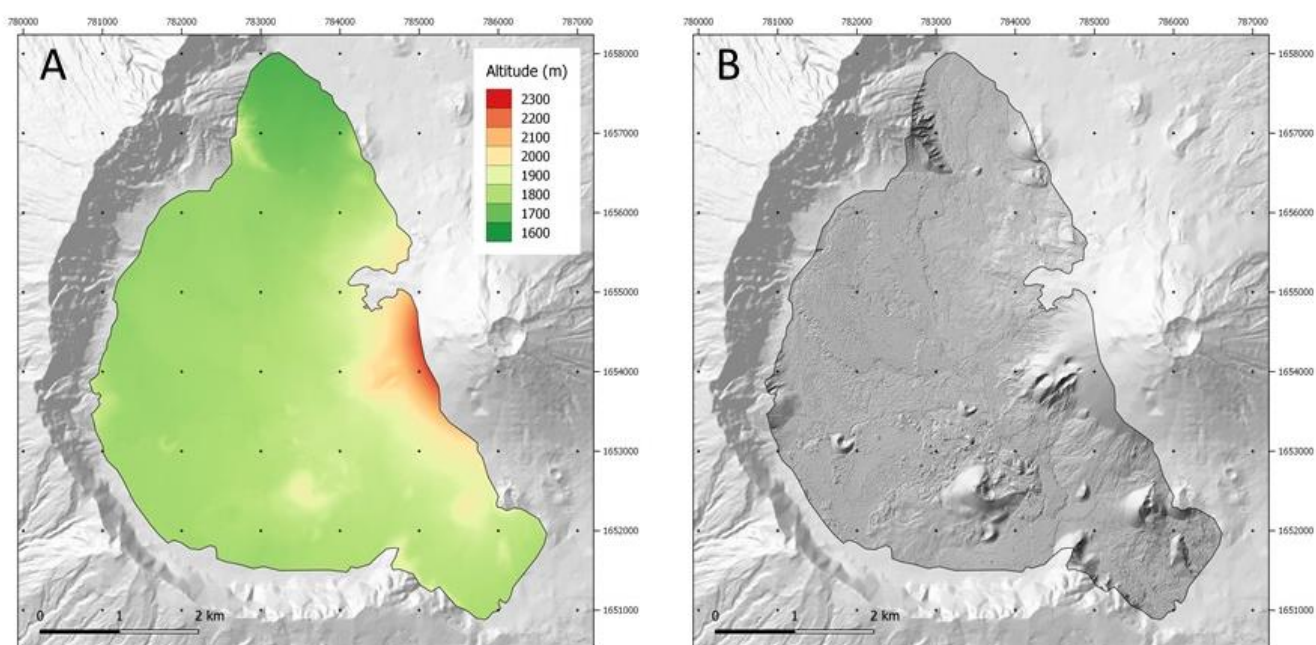
340 **Table 1 – Location accuracy per Ground Control Point in X, Y and Z.**

Check Point	ErrorX (m)	Error Y (m)	Error Z (m)	Projection Error (pixel)
beco03	-0.0218	-0.0110	0.0729	1.02
beco05	-0.1511	-0.1224	-0.0617	0.40
beco10	-0.0597	0.0347	0.2638	0.45
beco23	-0.0026	0.0791	0.0287	0.39
beco24	-0.0076	0.0844	0.1193	0.53
beco26	0.0286	0.1193	-0.0298	0.52
beco28	0.0671	0.0423	-0.0542	0.28
beco29	-0.0872	-0.0194	-0.1591	0.54
amarelo03	-0.0451	-0.1036	0.0280	0.41
amarelo05	-0.1162	-0.3011	0.2447	0.80
amarelo13	0.0567	0.0098	-0.1135	0.97
amarelo14	0.1900	0.0138	0.1076	0.74
amarelo16	-0.0011	0.1119	0.0940	0.60
Mean (m)	-0.0107	-0.0045	0.039	
RMSE (m)	0.082	0.107	0.125	



4.2 Digital Surface Model

345 The DSM of the Chã das Caldeiras with 25 cm resolution shows unprecedented topographic detail and allows for excellent visualization and quantification of the terrain morphometry. The iterative improvement of the point cloud by a detailed visual analysis of the DSM shaded relief model followed by adding almost 700 manual tie points in the model and reprocessing, allowed to reach a very high-quality result (Fig. 6). The final model is the result of a resampling of the first model obtained with 10 cm resolution.



350

Figure 6 – Digital surface model of the Chã das Caldeiras (A) and DSM shaded relief model (B). The surveyed area is overlaying the DEMFI (2010) 5 m DEM.

In order to guarantee the quality of its use, the DSM was divided in three quality zones (Fig. 7). The zonation is available in
355 the dataset as a shapefile that can be used to mask the DSM depending on user needs. The high resolution (10 cm) shaded relief model derived from the DSM, as well as the 50 cm equidistance contours interpolated from the DSM were used for the systematic visual analysis and for manual delineation of the areas with errors in the DSM.

360

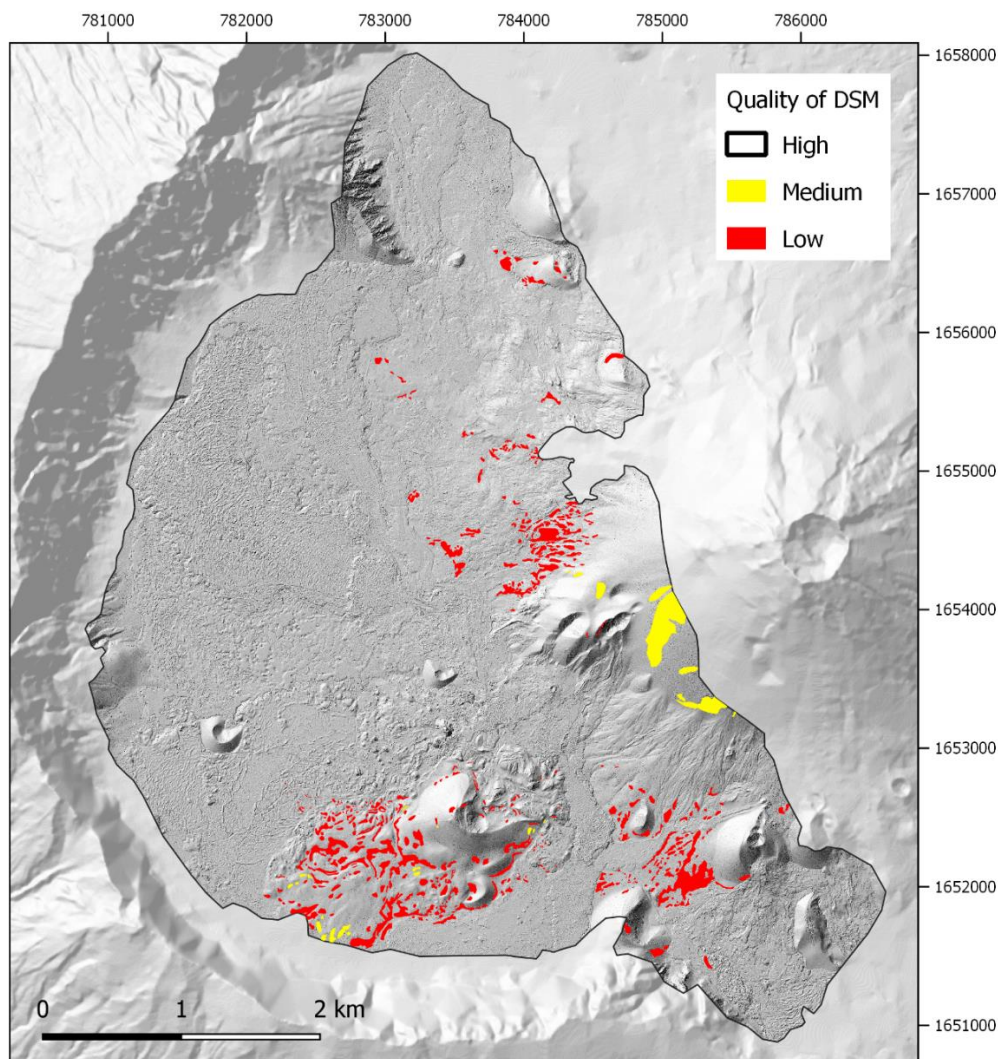


Figure 7 – Quality of the digital surface model in the Chã das Caldeiras. Shaded relief outside the surveyed area derived from the DEMFI (2010) 5 m DEM.

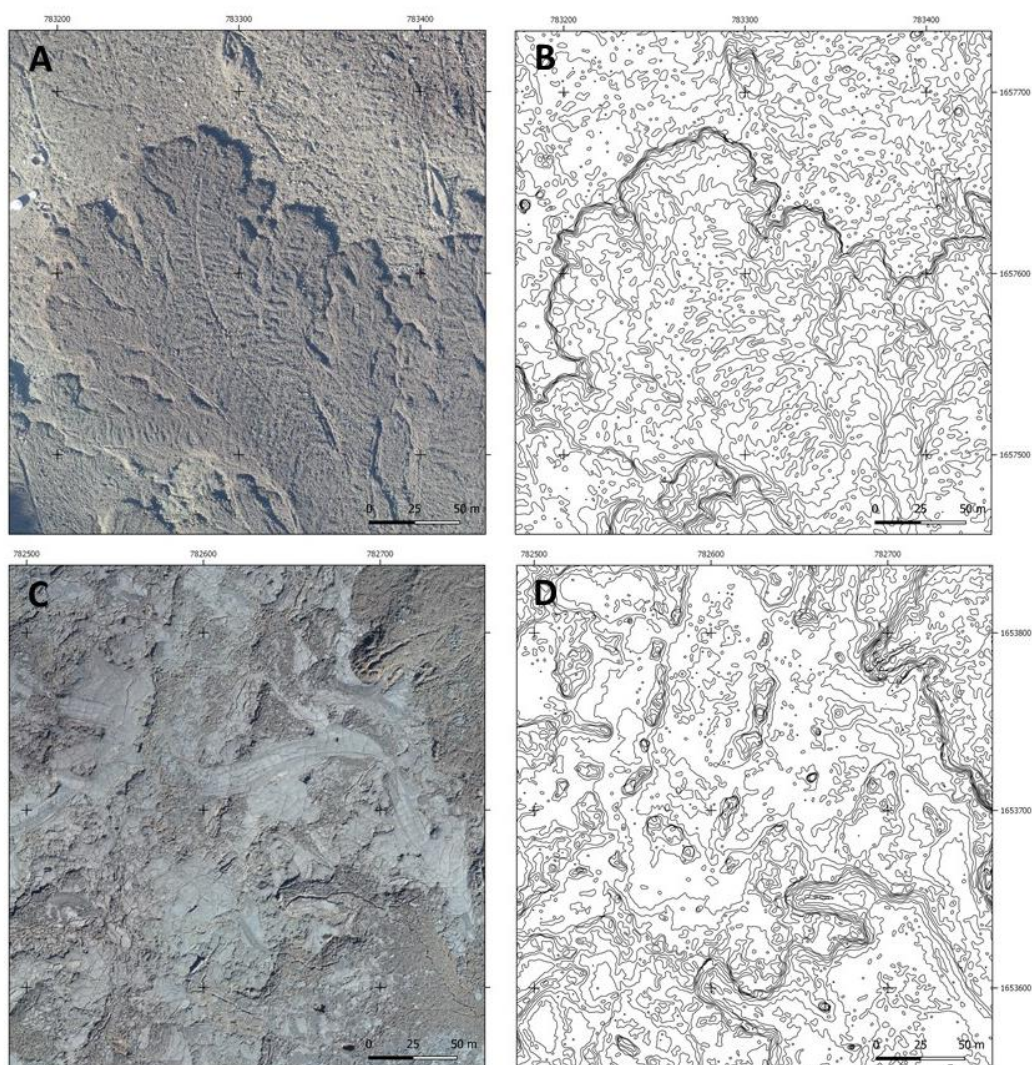
365

The high-quality zones cover 96.8% of the entire survey and coincide with areas of rough surfaces with numerous automatic and manual tie points, where the morphology is very accurate, and the point cloud model has high resolution. Figure 8 shows some selected examples of the types of surface present in the survey area, which allow to visually assess the quality of the model:

370 - The 'a'ā lava flow fields are characterized by high rugosity and numerous features which are easily matched between aerial photographs, including blocks, frequent sharp slope changes and pressure ridges (Figs. 8-A and 8-B).

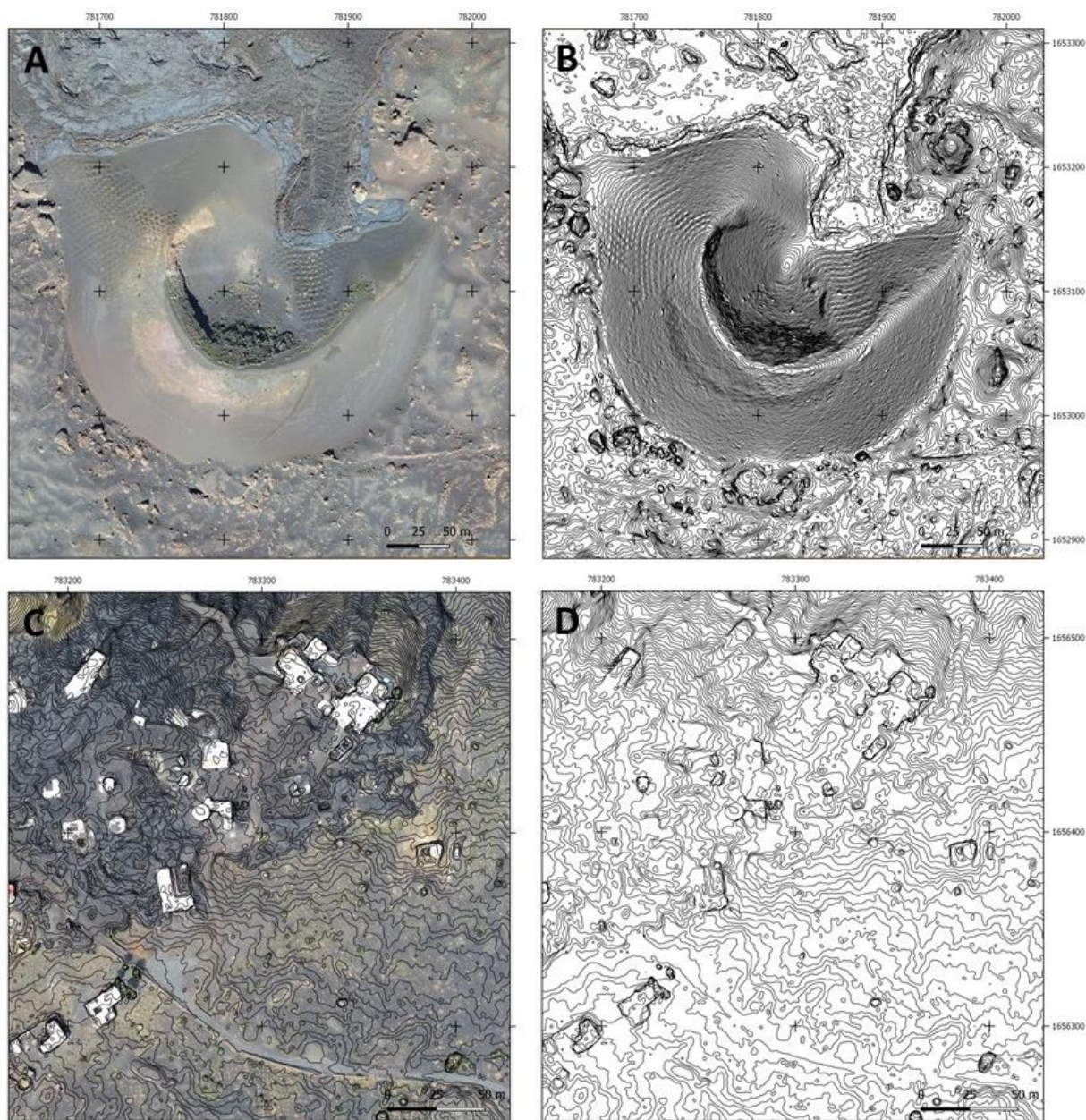


- Pāhoehoe lava flows show a much smoother and homogeneous surface, but they have frequent fractures and lineaments. They occupy generally small sectors of the orthomosaic and are bound by very rough a'ā lavas, facilitating point matching (Figs. 8-C and 8-D).
- 375 - Small volcanic cones with rough surfaces (e.g. boulders, footpaths, lava outcrops) show very high-quality results (Figs. 9-A and 9-B).
- Infrastructure, such as non-paved roads and houses show numerous matches and provide very accurate results. Cultivated areas occupy small sectors of the surveyed area, but the small holes dug to cultivate vines, as well as other small trees, are also very well represented in the DSM (Figs. 9-C and 9-D).



380

Figure 8 – Examples of surfaces in the Chã das Caldeiras with high-quality results for the digital surface model, with orthomosaic for visualization (10 cm resolution) and contour lines derived from the digital surface model (50 cm equidistance). Note the good quality of the elevation contours. A and B. ‘a’ā lava flows, C and D. Pāhoehoe lava field.



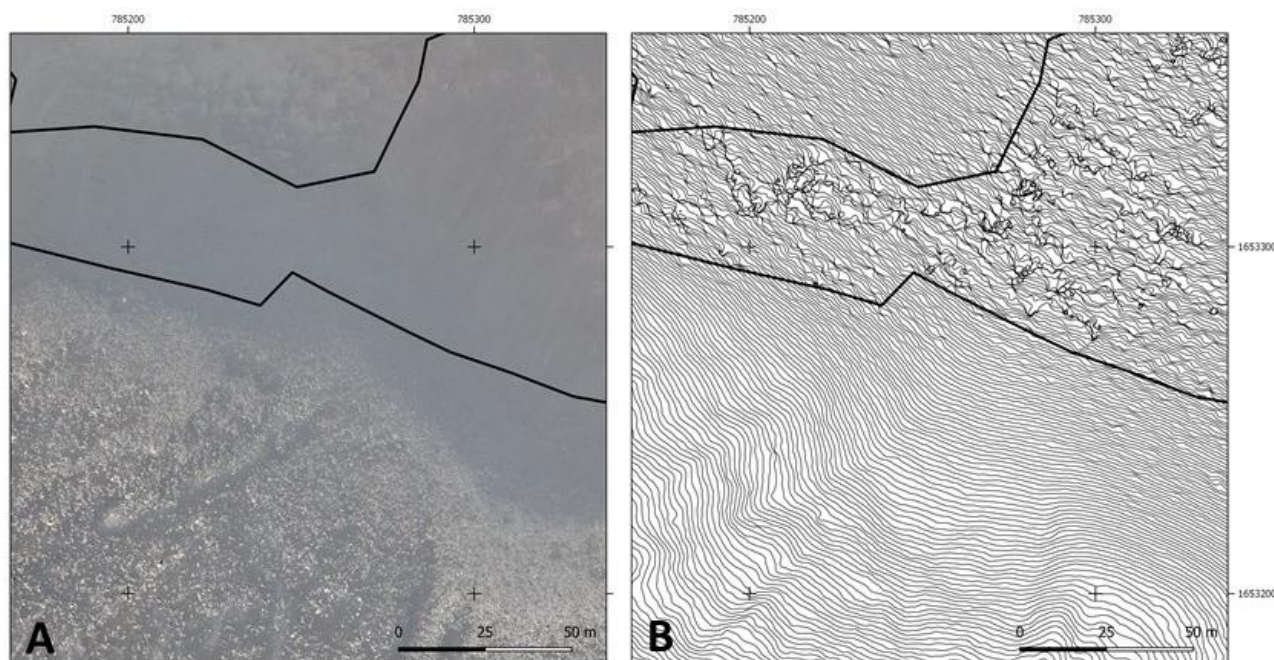
385

Figure 9 – Examples of surfaces in the Chã das Caldeiras with high-quality results for the digital surface model, with orthomosaic for visualization (10 cm resolution) and contour lines derived from the digital surface model (50 cm equidistance). Note the good quality of the elevation contours. A and B. Volcanic cone with cultivated areas inside the crater, C and D. Lava field with buildings and a road.

390



The medium-quality zones are sectors dominated by ash and lapilli, where sporadic 3D errors occur and occupy 0.6% of the survey. These areas, which in general can be used for visualization purposes and even for quantification, but with special care. Most errors in these zones are very small (dm scale) and can be smoothed by resampling, for example to 1-2 m resolution (Fig. 10).

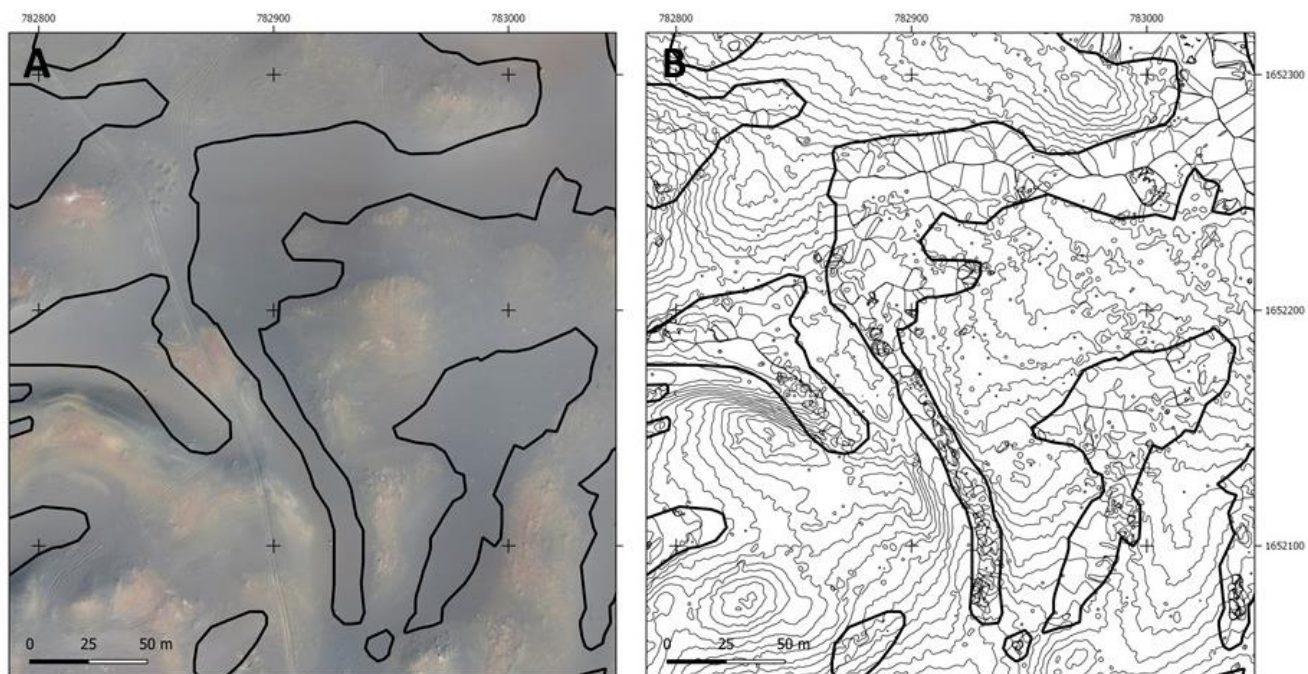


395

Figure 10 – Steep slope covered with ash in the Chã das Caldeiras with medium-quality results for the digital surface model. A. orthomosaic (10 cm resolution), and B. contour lines derived from the digital surface model (50 cm equidistance). The black line shows the boundary of the medium-quality area. The contours are very irregular in detail, but the overall slope at a coarse resolution is maintained. The area where the deposits are coarser provide a good DSM.

400

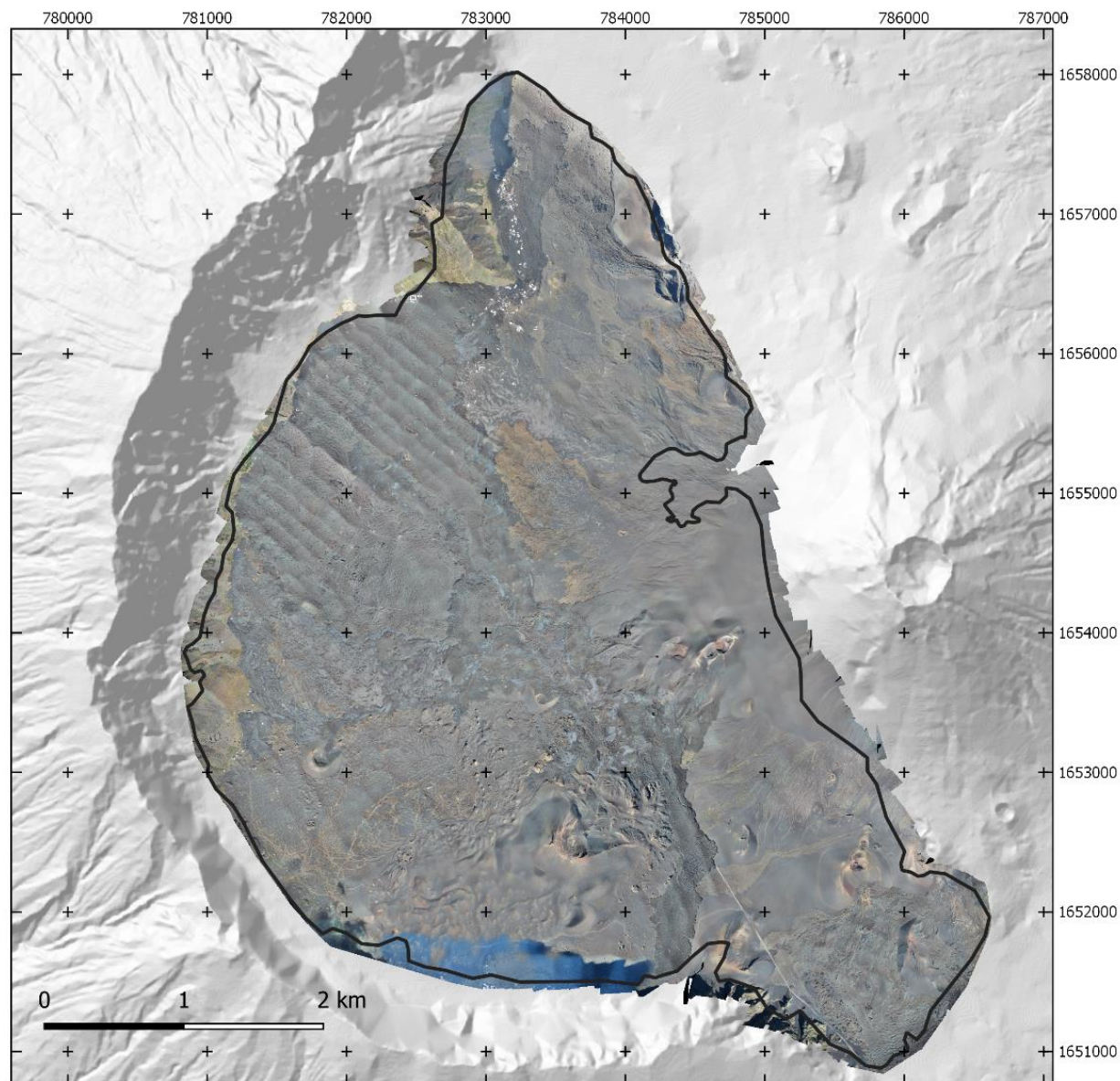
The low-quality zones correspond to patches where the point cloud was poorly resolved, having numerous artefacts in the DSM (Fig. 11). These areas cannot be used for quantification purposes and their visualization shows errors, which sometimes are significant. The low-quality zones only occupy 2.6% of the survey area. These cases occur in very smooth surfaces of ash and lapilli or in sectors where a small number of overlapping aerial photos exists. They are located mainly in
405 the base of some slopes, concave areas and also in the top of Monte Beco, due to the lack of photo overlapping.



410 **Figure 11 – Irregular surfaces with linear depressions covered with ash in the Chã das Caldeiras with poor-quality results for the digital surface model. A. orthomosaic for visualization (10 cm resolution), and B. contour lines derived from the digital surface model (50 cm equidistance). The black line shows the boundary of the low-quality area. The contours are very irregular and show numerous errors. The border with the good quality areas is sharp with good topography where the ground surface is coarser.**

4.3 Orthophoto mosaic

415 The digital orthophoto mosaic that shows a resolution of 25 cm (Fig. 12), but the high accuracy of the survey allowed to make a mosaic with a resolution of 10 cm. This product may be delivered upon request. The mosaic shows an overall high graphic quality, with few problems relating to shadow effects close to the Bordeira wall in the south of the Chã das Caldeiras, and with varying illumination conditions in the lava flows of the northwest part of the survey, where stripping occurs. The sectors with medium quality in the DSM do not affect the overall quality of the ortho mosaic, but the interpolation may result in geometrical inaccuracies in the orthophoto mosaic in the areas of low quality in the DSM.



420

Figure 12 – Digital orthophoto mosaic with 25 cm resolution of the Chã das Caldeiras. Shaded relief outside the surveyed area derived from the DEMFI (2010) 5 m DEM.

4.4 3D models for visualization

425 A 3D texture mesh (.fbx) was produced for visualization purposes, allowing for the accurate visualization of the whole surveyed area (Fig. 13).



Figure 13 – 3D visualization of the texture mesh of the Chã das Caldeiras.

430 **4.5 New estimates of the 2014-15 lava flow field area**

The lava flow field of the 2014-15 eruption was digitized manually using the orthomosaic and DSM. Unfortunately, our survey missed a small area of the lava flow with 0.007 km² in the northwest sector of Chã das Caldeiras, close to Monte Amarelo and that sector had to be digitised using very high-resolution Google Earth imagery. The accuracy of the present survey allowed to calculate a new area for the 2014-15 lava flow field, which is 4.53 km², a number smaller than the areas
435 calculated by other authors using coarser resolution imagery, that varied from 4.8 to 4.97 km² (5.8% to 8.9%). This discrepancy can be explained by the higher spatial resolution of our dataset that allows more accurate delineations, identifying in addition several kīpukas, i.e. small ‘islands’ (interior elevations surrounded by lava during the 2014-15 eruption) and also to a spatial variation effect (Chen, 1999) that results from the computation of the same areas in products with different spatial resolutions.

440 **5. Data availability**

The data is available at Zenodo: Vieira, Gonçalo, Mora, Carla, Pina, Pedro, Ramalho, Ricardo, & Fernandes, Rui. (2020). Digital surface model and orthomosaic of the Chã das Caldeiras lava fields (Fogo Island, Cape Verde, December 2016) (Version 1.0.0) [Data set]. Zenodo. <http://doi.org/10.5281/zenodo.4035038>.



The dataset consists of the following files:

- 445 - cha_caldeiras_contours_50cm.zip: Compressed shapefile (shp) and auxiliary files. Contour lines of the Chã das Caldeiras in December 2016 with 50 cm equidistance, interpolated from the digital surface model. CRS: ESPG 32626 - WGS 84 / UTM Zone 26N, elevation: ellipsoidal ITRF2014 (WGS84).
- cha_caldeiras_dsm_25cm.tif: Digital surface model of the Chã das Caldeiras in December 2016 with 25 cm resolution. CRS: ESPG 32626 - WGS 84 / UTM Zone 26N, elevation: ellipsoidal ITRF2014 (WGS84).
- 450 - cha_caldeiras_error_assessment_areas.zip: Compressed shapefile (shp) and auxiliary files. Areas with errors in the point cloud obtained by visual analysis. 1. Low accuracy, 2. Moderate accuracy. CRS: ESPG 32626 - WGS 84 / UTM Zone 26N.
- cha_caldeiras_ortho_25cm.tif: Orthomosaic RGB of the Chã das Caldeiras in December 2016 with 25 cm resolution. CRS: ESPG 32626 - WGS 84 / UTM Zone 26N.
- cha_caldeiras_pix4d_report.pdf: Report of the processing of the aerial imagery in PIX4D.
- 455 - lava-2014-15.zip: Compressed shapefile (shp) and auxiliary files. Lava flows of the eruption of 2014-15 digitised from the original 10 cm resolution orthomosaic. CRS: ESPG 32626 - WGS 84 / UTM Zone 26N.

6. Conclusions

The 23.9 km² very high-resolution digital surface model and orthophoto mosaic of the Chã das Caldeiras lava fields developed from UAV surveys of December 2016, show unprecedented detail and accuracy (resolution = 25 cm and RMSE =

460 0.103 m). 96.8% of the survey area has provided a very high-quality DSM, which due to the scarce vegetation and built areas may be used as a DEM. The areas with moderate problems occupy 0.6% of the survey, with only 2.6% of the area showing poor-quality. The sectors with problems in the point cloud and DSM are those associated to very homogeneous ash and lapilli deposits. These areas can be easily masked out of the DSM by using the shapefiles made available in the dataset. The rough surface 'a'ã lavas and the smooth pãhoehoe flows are very accurately determined, as well as the volcanic cones. The

465 resulting DSM and orthomosaic constitute base datasets of unprecedent detail of high-value for geological research and for lava flow modelling with a high potential for applications in risk mitigation. These products allow delineating accurately the borders between different surfaces (lava types and other classes) and perceiving sub-meter surface features, which is less accurate or not achievable at all at meter scale, over an area of several square kilometres. These morphometrics features include pressure ridges, tumuli, flow channels, levées, dragged blocks and remains of human structures, among other smaller

470 features.

Finally, we consider that these highly detailed products can play a relevant role in the assessment of volcanic hazards and related research and whose importance is surely excelled by becoming open access.



Acknowledgements

This research was conducted in the framework of the project FIRE – Fogo Island Volcano: multidisciplinary research on the
475 2014 eruption (FCT - PTDC/GEO-GEO/1123/2014) funded by the Fundação para a Ciência e a Tecnologia. R. Ramalho
acknowledges his IF/01641/2015 contract funded by FCT. The project 3DAntártida funded the acquisition of the UAV. The
INGT – Instituto Nacional de Gestão do Território and INMG – Instituto Nacional de Meteorologia e Geofísica de Cabo
Verde are thanked for their cooperation. Pedro Almeida, Carla Candeias, Stéphanie Dumont, Bento Martins and Carlos
Oliveira are thanked for their support in the collection of ground control points. Carlos Oliveira, Bruno Faria, Euda Miranda,
480 Fátima Fernandes and Jair Rodrigues are thanked for their support to the project and field activities. Co-funding by FCT I.P.
UIDB/00295/2020 – CEG and UIDP/00295/2020 - CEG, FCT - UIDB/50019/2020 – IDL and C4G – POCI-01-0145-
FEDER-022151.

Author contributions

GV, CM, PP and RR prepared the UAV survey planning and wrote the manuscript. GV and CM conducted the UAV
485 surveys. PP and RR conducted the GNSS GCP collection. GV and CM conducted the modelling. RR digitised the lava
flows. RF coordinated the GNSS activities. All authors contributed to discussion and review of the manuscript.

References

- Amici, S., Turci, M., Giammanco, S., Spampinato, L., and Giulietti, F.: UAV thermal infrared remote sensing of an Italian
mud volcano, *Adv. Remote Sens.*, 02, 04, 358–364, <http://dx.doi.org/10.4236/ars.2013.24038>, 2013.
- 490 Bagnardi, M., González, P. J., and Hooper, A.: High-resolution digital elevation model from tri-stereo Pleiades-1 satellite
imagery for lava flow volume estimates at Fogo volcano: tri-stereo Pleiades DEM of Fogo volcano, *Geophysical Research
Letters* 43, <http://dx.doi.org/10.1002/2016GL06945>, 2016.
- Baldi, P., Bonvalot, S., Briole, P., Coltelli, M., Gwinner, K., Marsella, M., Puglisi, G., and Rémy, D.: Validation and
comparison of different techniques for the derivation of digital elevation models and volcanic monitoring (Vulcano Island,
495 Italy), *Int. J. Remote Sens.*, 23, 22, 4783–4800. <https://doi.org/10.1080/01431160110115861>, 2002.
- Barrett, R., Lebas, E., Ramalho, R., Klauke, I., Kutterolf, S., Klügel, A., Lindhorst, K., Gross, F., and Krastel, S.: Revisiting
the tsunamigenic volcanic flank-collapse of Fogo Island in the Cape Verdes, offshore West Africa. Geological Society,
London, Special Publications, 500, <https://doi.org/10.1144/SP500-2019-187>, 2019.
- Bebiano, J.: A geologia do arquipélago de Cabo Verde. *Comunicações dos Serviços Geológicos de Portugal*, 18, 167–187,
500 1932.



- Benoit, L., Gourdon, A., Vallat, R., Irarrazaval, I., Gravey, M., Lehmann, B., Prasicek, G., Gräff, D., Herman, F., and Mariethoz, G.: A high-resolution image time series of the Gorner Glacier – Swiss Alps – derived from repeated unmanned aerial vehicle surveys, *Earth Syst. Sci. Data*, 11, 579–588, <https://doi.org/10.5194/essd-11-579-2019>, 2019.
- Bignami, C., Chini, M., Amici, S. and Trasatti E.: Synergic use of multi-sensor satellite data for volcanic hazards monitoring: the Fogo (Cape Verde) 2014-2015 effusive eruption, *Frontiers of Earth Science*, 8, 22, <https://doi.org/10.3389/feart.2020.00022>, 2020.
- Bonali, F. L., Tibaldi, A., Marchese, F., Fallati, L., Russo, E., Corselli, C., and Savini, A.: UAV-based surveying in volcano-tectonics: An example from the Iceland rift, *Journal of Structural Geology*, 121, 46–64, <https://doi.org/10.1016/j.jsg.2019.02.004>, 2019.
- 510 Brum da Silveira, A., Madeira, J., and Serralheiro, A.: A estrutura da Ilha do Fogo, Cabo Verde. A Erupção Vulcânica de 1995 na Ilha do Fogo, Cabo Verde. Publ. IICT, Lisboa, 63–78, 1997a.
- Brum da Silveira, A., Madeira, J., Serralheiro, A., Torres, P.C., Silva, L.C., and Mendes, M. H.: O controlo estrutural da erupção de Abril de 1995 na Ilha do Fogo, Cabo Verde. A Erupção Vulcânica de 1995 na Ilha do Fogo, Cabo Verde. Publ. IICT, Lisboa, 51–61, 1997b.
- 515 Brunier, G., Fleury, J., Anthony, E. J., Gardel, A., and Dussouillez, P.: Close-range airborne Structure-from-Motion Photogrammetry for high-resolution beach morphometric surveys: Examples from an embayed rotating beach, *Geomorphology*, 261, 76–88, <http://doi.org/10.1016/j.geomorph.2016.02.025>, 2016.
- Bühler, Y., Adams, M. S., Bösch, R., and Stoffel, A.: Mapping snow depth in alpine terrain with unmanned aerial systems (UAS): potential and limitations. *The Cryosphere*, 10, 1075-1088, <https://doi.org/10.5194/tc-10-1075-2016>, 2016.
- 520 Burke, K., and Wilson, J.T.: Is the African plate stationary? *Nature*, 239, 5372, 387-390, <https://doi.org/10.1038/239387b0>, 1972.
- Campana, S.: Drones in Archaeology. State-of-the-art and Future Perspectives, *Archaeol. Prospect*, 24, 275–296, <https://doi.org/10.1002/arp.1569>, 2017.
- Cappello, A., Ganci, G., Calvari, S., Pérez, N. M., Hernández, P. A., Silva, S. V., Cabral, J., and Negro, C. D.: Lava flow hazard modeling during the 2014–2015 Fogo eruption, Cape Verde, *Journal of Geophysical Research: Solid Earth*, 121, 2290–2303, <https://doi.org/10.1002/2015JB012666>, 2016.
- 525 Chikhradze, N., Henriques, R., Elashvili, M., Kirkitadze, G., Janelidze, Z., Bolashvili, N., and Lominadze, G.: Close Range Photogrammetry in the Survey of the Coastal Area Geoecological Conditions (on the Example of Portugal), 4, 35–40, <http://doi.org/10.11648/j.earth.s.2015040501.17>, 2015.
- 530 Chio, S.-H. and Lin, C.-H.: Preliminary study of UAS equipped with thermal camera for volcanic geothermal monitoring in Taiwan, *Sensors*, 17, 1649, <https://doi.org/10.3390/s17071649>, 2017.
- Christiansen, P., Steen, K. A., Jorgensen, R. N., and Karstoft, H.: Automated detection and recognition of wildlife using thermal cameras, *Sensors*, 14, 13778–13793, <https://doi.org/10.3390/s140813778>, 2014.



- Colomina, I. and Molina, P.: Unmanned aerial systems for photogrammetry and remote sensing: A review, *ISPRS Journal of*
535 *Photogrammetry and Remote Sensing*, 92, 79–97, <http://dx.doi.org/10.1016/j.isprsjprs.2014.02.013>, 2014.
- Dąbski, M., Zmarz, A., Rodzewicz, M., Korczak-Abshire, M., Karsznia, I., Lach, K., Rachlewicz, G., and Chwedorzewska,
K.: Mapping glacier forelands based on UAV BVLOS operation in Antarctica, *Remote Sensing*, 12 ,4, 630,
<https://doi.org/10.3390/rs12040630>, 2020.
- Darmawan, H., Walter, T. R., Brotospito, K. S., Subandriyo, and Nandaka, I. G. M. A.: Morphological and structural
540 changes at the Merapi lava dome monitored in 2012–15 using unmanned aerial vehicles (UAVs), *Journal of Volcanology*
and Geothermal Research, 349, 256-267. <https://doi.org/10.1016/j.jvolgeores.2017.11.006>, 2018.
- Day, S. J., Heleno, S. I. N., and Fonseca, J. F. B. D.: A past giant lateral collapse and present-day flank instability of Fogo,
Cape Verde Islands. *Journal of Volcanology and Geothermal Research*, 94, 191-218, [https://doi.org/10.1016/S0377-0273\(99\)00103-1](https://doi.org/10.1016/S0377-0273(99)00103-1), 1999.
- 545 De Beni, E., Cantarero, M., and Messina, A.: UAVs for volcano monitoring: A new approach applied on an active lava flow
on Mt. Etna (Italy), during the 27 February–02 March 2017 eruption, *Journal of Volcanology and Geothermal Research*, 369,
250–262, <https://doi.org/10.1016/j.jvolgeores.2018.12.001>, 2019.
- de Moor, J. M., Stix, J., Avar, G., Muller, C., Corrales, E., Diaz, J. A., Alan, A., Brenes, J., Pacheco, J., Aiuppa, A., and
Fischer, T. P.: Insights on hydrothermal-magmatic interactions and eruptive processes at Poás volcano (Costa Rica) from
550 high-frequency gas monitoring and drone measurements, *Geophysical Research Letters*, 46, 1293–1302,
<https://doi.org/10.1029/2018GL08030>, 2019.
- Di Felice, F., Mazzini, A., Di Stefano, G., and Romeo, G.: Drone high resolution infrared imaging of the Lusi mud eruption,
Marine and Petroleum Geology, 90, 38-51, <http://dx.doi.org/10.1016/j.marpetgeo.2017.10.025>, 2018.
- Diefenbach, A. K., Bull, K. F., Wessels, R. L., and McGimsey, R. G.: Photogrammetric monitoring of lava dome growth
555 during the 2009 eruption of Redoubt Volcano, *J. Volcanol. Geotherm. Res.*, 259, 308–316,
<https://doi.org/10.1016/j.jvolgeores.2011.12.009>, 2013.
- Eisele, S., Reißig, S., Freundt, A., Kutterolf, S., Nürnberg, D., Wang, K.L., and Kwasnitschka, T.: Pleistocene to Holocene
offshore tephrostratigraphy of highly explosive eruptions from the southwestern Cape Verde Archipelago, *Marine Geology*,
369, 233-250, <https://doi.org/10.1016/j.margeo.2015.09.006>, 2015.
- 560 Faria, B. and Fonseca, J. F. B. D.: Investigating volcanic hazard in Cape Verde Islands through geophysical monitoring:
network description and first results, *Natural Hazards and Earth System Sciences*, 14, 485–499,
<https://doi.org/10.5194/nhess-14-485-2014>, 2014.
- Favalli, M., Fornaciai, A., Nannipieri, L., Harris, A., Calvari, S., and Lormand C.: UAV-based remote sensing surveys of
lava flow fields: a case study from Etna’s 1974 channel-fed lava flows, *Bulletin of Volcanology*, 80, 29.
565 <https://doi.org/10.1007/s00445-018-1192-6>, 2018.
- Favalli, M., Fornaciai, A., and Pareschi, M.T.: LIDAR strip adjustment: Application to volcanic areas, *Geomorphology*, 111,
3, 123–135, <https://doi.org/10.1016/j.geomorph.2009.04.010>, 2009.



- Fonseca, J., Flor, A., Goncalves, A., Day, S., Jenkyns, S.: Perigosidade vulcânica das ilhas de Cabo Verde, in: Riscos geológicos das ilhas de Cabo Verde, Municipia Final Report to Cape Verde UNDP Office, edited by Mileu, N., Lisbon, 570 2014.
- Fornaciai, A., Bisson, M., Landi, P., Mazzarini, F., and Pareschi, M.T.: A LiDAR survey of Stromboli volcano (Italy): Digital elevation model-based geomorphology and intensity analysis, *Int. J. Remote Sens.*, 31, 12, 3177–3194, <https://doi.org/10.1080/01431160903154416>, 2010.
- Gomez, C. and Purdie, H.: UAV- based photogrammetry and geocomputing for hazards and disaster risk monitoring – A 575 review, *Geoenvironmental Disasters*, 3, 23, <http://doi.org/10.1186/s40677-016-0060-y>, 2016.
- González, P. J., Bagnardi, M., Hooper, A.J., and Larsen, Y., Marinkovic, P., Samsonov, S.V., Wright, T.J.: The 2014–2015 eruption of Fogo volcano: Geodetic modeling of Sentinel-1 TOPS interferometry, *Geophysical Research Letters*, 42, 21, 9239–9246, <https://doi.org/10.1002/2015GL066003> 2015.
- Hassan-Esfahani, L., Torres-Rua, A., Jensen, A., and McKee, M.: Assessment of surface soil moisture using high-resolution 580 multi-spectral imagery and artificial neural networks, *Remote Sens.*, 7, 2627–2646, <https://doi.org/10.3390/rs70302627>, 2015.
- Hassler, S. C. and Baysal-Gurel, F.: Unmanned Aircraft System (UAS) technology and applications in agriculture, *Agronomy*, 9, 618, <https://doi.org/10.3390/agronomy9100618>, 2019.
- Heleno da Silva, S.I.N., Day, S.J., and Fonseca, J.F.B.D.: Fogo Volcano, Cape Verde Islands: seismicity-derived constraints 585 on the mechanism of the 1995 eruption, *J. Volcanol. Geotherm. Res.*, 94, 219–231, [https://doi.org/10.1016/S0377-0273\(99\)00104-3](https://doi.org/10.1016/S0377-0273(99)00104-3), 1999.
- Jenkins, S. F., Day, S. J., Faria, B.V.E., and Fonseca, J. F. B. D.: Damage from lava flows: insights from the 2014–2015 eruption of Fogo, Cape Verde, *Journal of Applied Volcanology*, 6, 1, 1–17, <https://doi.org/10.1186/s13617-017-0057-6>, 2017.
- 590 Jordan, B.R.: Collecting field data in volcanic landscapes using small UAS (sUAS)/drones, *Journal of Volcanology and Geothermal Research*, 385, 231–241, <https://doi.org/10.1016/j.jvolgeores.2019.07.006>, 2019.
- Jouvet, G., Dongen, E., Lüthi, M.P., and Vieli, A.: In situ measurements of the ice flow motion at Eqip Sermia Glacier using a remotely controlled unmanned aerial vehicle (UAV), *Geosci. Instrum. Method. Data Syst.*, 9, 1–10, <https://doi.org/10.5194/gi-9-1-2020>, 2020.
- 595 Kattenborn, T., Sperlich, M., Bataua, K., and Koch, B.: Automatic Single Tree Detection in Plantations using UAV-based Photogrammetric Point clouds. *ISPRS – International Archives of the Photogrammetry, Remote Sensing and Spatial Information Sciences*, XL- 3(September), 139–144. <http://doi.org/10.5194/isprsarchives-XL-3-139-2014>, 2014.
- Kerle, N.: Volume estimation of the 1998 flank collapse at Casita volcano, Nicaragua: A comparison of photogrammetric and conventional techniques, *Earth Surf. Processes Landforms*, 27, 7, 759–772, <https://doi.org/10.1002/esp.351>, 2002.
- 600 Komorowski, J. C., Morin, J., Jenkins, S., and Kelman, I.: Challenges of Volcanic Crises on Small Islands States. In: Fearnley C.J., Bird D.K., Haynes K., McGuire W.J., Jolly G. (eds) *Observing the Volcano World. Advances in Volcanology*



- (An Official Book Series of the International Association of Volcanology and Chemistry of the Earth's Interior – IAVCEI, Barcelona, Spain). Springer, https://doi.org/10.1007/11157_2015_15, 2016.
- Le Bas, T. P., Masson, D.G., Holtom, R. T. and Grevemeyer, I.: Slope failures of the flanks of the southern Cape Verde Islands. In: Lykousis, V., Sakellariou, D. and Locat, J. (eds) *Submarine Mass Movements and Their Consequences. Advances in Natural and Technological Hazards Research*, 27. Springer, Dordrecht, 337–345, https://doi.org/10.1007/978-1-4020-6512-5_35, 2007.
- Lindgren, P. R., Grosse, G., Walter, Anthony K. M., and Meyer, F. J.: Detection and spatiotemporal analysis of methane ebullition on thermokarst lake ice using high-resolution optical aerial imagery, *Biogeosciences*, 13, 27–44, <https://doi.org/10.5194/bg-13-27-2016>, 2016.
- Liu, E.J., Wood, K., Mason, E., Edmonds, M., Aiuppa, A., Giudice, G., Bitetto, M., Francofonte, V., Burrow, S., Richardson, T., Watson, M., Pering, T. D., Wilkes, T.C., McGonigle, A. J. S., Velasquez, G., Melgarejo, C., and Bucarey C.: Dynamics of outgassing and plume transport revealed by proximal unmanned aerial system (UAS) measurements at Volcán Villarrica, Chile. *Geochemistry, Geophysics, Geosystems*, 20, 730–750, <https://doi.org/10.1029/2018GC007692>, 2019.
- Lodge, A. and Helffrich, G.: Depleted swell root beneath the Cape Verde Islands, *Geology*, 34, 6, 449–452, <https://doi.org/10.1130/G22030.1>, 2006.
- Long, N., Millescamp, B., Guillot, B., Pouget, F., and Bertin, X.: Monitoring the Topography of a Dynamic Tidal Inlet Using UAV Imagery, *Remote Sens.*, 8, 387, <https://doi.org/10.3390/rs8050387>, 2016.
- Lucieer, A., de Jong, S. M., and Turner, D.: Mapping landslide displacements using Structure from Motion (SfM) and image correlation of multi-temporal UAV photography, *Progress in Physical Geography*, 38, 1, 97–116. <http://doi.org/10.1177/0309133313515293>, 2014.
- Machado, F. and Torre de Assunção, C. F.: Carta geológica de Cabo Verde na escala de 1/100,000.; noticia explicativa da folha da ilha do Fogo — estudos petrográficos. Garcia de Orta, Lisboa. 13, 597–604, 1965.
- Madeira, J., Brum da Silveira, A., Mata, J., Mourão, C., and Martins, S.: The role of mass movements on the geomorphologic evolution of island volcanoes: examples from Fogo and Brava in the Cape Verde archipelago, *Comunicações Geológicas*, 95, 93–106, 2008.
- Madeira, J., Ramalho, R. S., Hoffmann, D. L., Mata, J., and Moreira, M.: A geological record of multiple Pleistocene tsunami inundations in an oceanic island: The case of Maio, Cape Verde, *Sedimentology*, 67, 1529–1552, <https://doi.org/10.1111/sed.12612>, 2020.
- Major, J.J., Dzurisin, D., Schilling, S. P., and Poland, M. P.: Monitoring lava-dome growth during the 2004–2008 Mount St. Helens, Washington, eruption using oblique terrestrial photography, *Earth Planet. Sci. Lett.*, 286, 1–2, 243–254, <https://doi.org/10.1016/j.epsl.2009.06.034>, 2009.
- Masson, D.G., Le Bas, T. P., Grevemeyer, I., and Weinrebe, W.: Flank collapse and large-scale landsliding in the Cape Verde Islands, off West Africa, *Geochemistry, Geophysics, Geosystems*, 9, 16, <https://doi.org/10.1029/2008GC001983>, 2008.



- Mata, J., Martins, S., Mattielli, N., Madeira, J., Faria, B., Ramalho, R., Silva, P., Moreira, M., Caldeira, R., Moreira, M., Rodrigues, J., and Martins, L.: The 2014–15 eruption and the short-term geochemical evolution of the Fogo volcano (Cape Verde): Evidence for small-scale mantle heterogeneity, *Lithos*, 288–289, 91–107, <https://doi.org/10.1016/j.lithos.2017.07.001>, 2017.
- 640 Mazzarini, F. M. T. Pareschi, M. Favalli, I. Isola, S. Tarquini, and E. Boschi.: Lava flow identification and aging by means of lidar intensity: Mount Etna case, *J. Geophys. Res.*, 112, B02201, <https://doi.org/10.1029/2005JB004166>, 2007.
- McGonigle, A. J. S., Aiuppa, A., Giudice, G., Tamburello, G., Hodson, A.J., and Gurrieri, S.: Unmanned aerial vehicle measurements of volcanic carbon dioxide fluxes, *Geophys. Res. Lett.*, 35, 6, L06303, <https://doi.org/10.1029/2007GL032508>, 2008.
- 645 Miranda, V., Pina, P., Heleno, S., Vieira, G., Mora, C., and Schaefer, C. E. G. R.: Monitoring recent changes of vegetation in Fildes Peninsula (King George Island, Antarctica) through satellite imagery guided by UAV surveys, *Science of The Total Environment*, 704, 135295, <https://doi.org/10.1016/j.scitotenv.2019.135295>, 2020.
- Mora, C., Vieira, G., Pina, P., Lousada, M., and Christiansen, H. H.: Land Cover Classification Using High-Resolution Aerial Photography in Adventdalen, Svalbard, *Geografiska Annaler: Series A, Physical Geography*, 97, 3, 473–488, <http://doi.org/10.1111/geoa.12088>, 2015.
- 650 Mori, T., Hashimoto, T., Terada, A., Yoshimoto, M., Kazahaya, R., Shinohara, H., and Tanaka, R.: Volcanic plume measurements using a UAV for the 2014 Mt. Ontake Eruption, *Earth Planets Space*, 68–49, <https://doi.org/10.1186/s40623-016-0418-0>, 2016.
- Mouginis-Mark, P. J., and Garbeil, H.: Quality of TOPSAR topographic data for volcanology studies at Kīlauea Volcano, Hawaii: An assessment using airborne lidar data, *Remote Sens. Environ.*, 96, 2, 149–164, <https://doi.org/10.1016/j.rse.2005.01.017>, 2005.
- Müller, D., Walter, T.R., Schöpa, A., Witt, T., Steinke, B., Gudmundsson, M.T., and Dürig, T.: High-resolution digital elevation modeling from TLS and UAV campaign reveals structural complexity at the 2014/2015 Holuhraun eruption site, Iceland, *Front. Earth Sci.*, 5, 59, <https://doi.org/10.3389/feart.2017.00059>, 2017.
- 660 Nakano, T., Kamiya, I., Tobita, M., Iwahashi, J., and Nakajima, H.: Landform monitoring in active volcano by UAV and SfM-MVS technique. *The International Archives of the Photogrammetry, Remote Sensing and Spatial Information Sciences*, 40, 8, 71–75, <https://doi.org/10.5194/isprsarchives-XL-8-71-2014>, 2014.
- Pajares, G.: Overview and current status of remote sensing applications based on Unmanned Aerial Vehicles (UAVs), *Photogrammetric Engineering & Remote Sensing*, 81,4, 281–330, <https://doi.org/10.14358/PERS.81.4.281>, 2015.
- 665 Paris, R., Geichetti, T., Chevalier, J., Guillou, H., and Frank, N.: Tsunami deposits in Santiago Island (Cape Verde archipelago) as possible evidence of a massive flank failure of Fogos volcano, *Sedimentary Geology*, 239, 129–145, <https://doi.org/10.1016/j.sedgeo.2011.06.006>, 2011.



- Paris, R., Ramalho, R.S., Madeira, J., Ávila, S., May, S.M., Rixhon, G., Engel, M., Brückner, H., Herzog, M., Schukraft, G., and Perez-Torrado, F.J.: Mega-tsunami conglomerates and flank collapses of ocean island volcanoes, *Marine Geology*, 395, 670 168–187, <https://doi.org/10.1016/j.margeo.2017.10.004>, 2018.
- Poland, M.P.: Time-averaged discharge rate of subaerial lava at K⁻īlauea Volcano, Hawai'i, measured from TanDEM-X interferometry: Implications for magma supply and storage during 2011–2013, *J. Geophys. Res. Solid Earth*, 119, 5464–5481, <https://doi.org/10.1002/2014JB011132>, 2014.
- Ramalho, R., Winckler, G., Madeira, J., Helffrich, G. Hipólito, A., Quartau, R., Adena, K., and Schaefer, J.: Hazard potential 675 of volcanic flank collapses raised by new megatsunami evidence, *Science Advances*, 1, 9, E1500456, <https://doi.org/10.1126/sciadv.1500456>, 2015.
- Ramalho, R. A. S. (Ed.): *Building the Cape Verde Islands*, 1st ed., Springer, Berlin, Heidelberg, 2011.
- Ramalho, R., Helffrich, D., Cosca, M., Vance, D., Hoffmann, D., and Schmidt, D. N.: Episodic swell growth inferred from variable uplift of the Cape Verde hotspot islands, *Nature Geoscience*, 3, 11, 774–777, <https://doi.org/10.1038/ngeo982>, 680 2010a.
- Ramalho, R., Helffrich, D., Cosca, M., Vance, D., Hoffmann, D., and Schmidt, D. N.: Vertical movements of ocean island volcanoes: Insights from a stationary plat. environment, *Marine Geology.*, 275, 84–95, <https://doi.org/10.1016/j.margeo.2010.04.009>, 2010b.
- Ramalho, R. S., Helffrich, G., Schmidt, D. N., and Vance, D.: Tracers of uplift and subsidence in the Cape Verde 685 Archipelago, *Journal of the Geological Society of London*, 167, 3, 519–538, doi:10.1144/0016-76492009-056, 2010c.
- Ribeiro, O.: *A ilha do Fogo e as suas erupções*. Comissão Nacional para as Comemorações dos Descobrimentos Portugueses, 1954.
- Richter, N., Favalli, M., Dalfsen, E. Z., Fornaciai, A., Fernandes, R. M. S., Rodriguez, N. P., Levy, J., Victória, S. S., and Walter, Th.R.: Lava flow hazard at Fogo volcano, Cape Verde, before and after the 2014–2015 eruption, *Natural Hazards and Earth Systems*, 16, 1925–1951, <https://doi.org/10.5194/nhess-16-1925-2016>, 2016. 690
- Risbøl, O. and Gustavsen, L.: LiDAR from drones employed for mapping archaeology – Potential, benefits and challenges, *Archaeological Prospection*, 25, 4, 329–338, <https://doi.org/10.1002/arp.1712>, 2018.
- Rowland, S. K., MacKay, M.E., Garbeil, H., and Mouginiis-Mark, P. J.: Topographic analyses of K⁻īlauea Volcano, Hawai'i, from interferometric airborne radar, *Bull. Volcanol.*, 61, 1–2, 1–14, doi:10.1029/2019GL083501, 1999.
- 695 Rüdiger, J., Tirpitz, J.-L., de Moor ,J.M., Bobrowski, N., Gutmann, A., Liuzzo, M., Ibarra ,M., and Hoffmann, T.: Implementation of electrochemical, optical and denuder-based sensors and sampling techniques on UAV for volcanic gas measurements: examples from Masaya, Turrialba and Stromboli volcanoes, *Atmospheric Measurement Techniques*, 11, 2441–2457, <https://doi.org/10.5194/amt-11-2441-2018>, 2018.
- 700 Salzer, J. T., Milillo, P., Varley, N., Perissin, D., Pantaleo, M., and Walter, T. R.: Evaluating links between deformation, topography and surface temperature at volcanic domes: results from a multi-sensor study at Volcán de Colima, Mexico, *Earth Planet. Sci. Lett.* 479, 354–365, <https://doi.org/10.1016/j.epsl.2017.09.027>, 2017.



- Smith, M. W., Carrivick, J. L., and Quincey, D. J.: Structure from motion photogrammetry in physical geography, *Progress in Physical Geography*, 40, 2, 247–275, <https://doi.org/10.1016/j.geomorph.2012.08.021>, 2016.
- Stevens, N., Wadge, G., and Murray, J.: Lava flow volume and morphology from digitised contour maps: A case study at
705 Mount Etna, Sicily, *Geomorphology*, 28, 3–4, 251–261, [https://doi.org/10.1016/S0169-555X\(98\)00115-9](https://doi.org/10.1016/S0169-555X(98)00115-9), 1999.
- Stix, J., de Moor, J. M., Rüdiger, J., Alan, A., Corrales, E., D’Arcy, F., Diaz, J. A., and Liotta, M.: Using drones and miniaturized instrumentation to study degassing at Turrialba and Masaya volcanoes, Central America, *Journal of Geophysical Research: Solid Earth*, 123, 6501–6520, <https://doi.org/10.1029/2018JB015655>, 2018.
- Thiele, S. T., Varley, N., and James, M. R.: Thermal photogrammetric imaging: a new technique for monitoring dome
710 eruptions, *J. Volcanol. Geotherm. Res.*, 337, 140–145, <https://doi.org/10.1016/j.jvolgeores.2017.03.022>, 2017.
- Torres, P. C., Madeira, J., Silva, L. C., Brum da Silveira, A., Serralheiro, A., and Mota Gomes, A.: Carta Geológica das Erupções Históricas da Ilha do Fogo (Cabo Verde): revisão e actualização, *Comunicações do Instituto Geológico e Mineiro* 84, A193–196, 1998.
- Turner, N. R., Perroy, R. L., and Hon, K.: Lava flow hazard prediction and monitoring with UAS: a case study from the
715 2014–2015 Pāhoa lava flow crisis, Hawai‘I, *Journal of Applied Volcanology*, 6, 17, <http://doi.org/10.1186/s13617-017-0068-3>, 2017.
- Vieira, D., Teodoro, A., and Gomes, A.: Analysing Land Surface Temperature variations during Fogo Island (Cape Verde) 2014–2015 eruption with Landsat 8 images, *Proc. of SPIE*, 10005, 1000508–14, 2016.
- Vieira, G., Mora, C., Pina, P., Ramalho, R., and Fernandes, R.: Digital surface model and orthomosaic of the Chã das
720 Caldeiras lava fields (Fogo Island, Cape Verde, December 2016) (Version 1.0.0) [Data set]. Zenodo. <http://doi.org/10.5281/zenodo.4035038>, 2020.
- Wakeford, Z. E., Chmielewska, M., Hole, M. J., Howell, J. A., and Jerram, D. A.: Combining thermal imaging with photogrammetry of an active volcano using UAV: an example from Stromboli, Italy, *Photogrammetric Record*, 34, 168, 445–466, <https://doi.org/10.1111/phor.12301>, 2019.
- 725 Walter, T. R., Ratdomopurbo, A., Subandriyo, N., Aisyah, K., Brotospito, S., Salzer, J., and Lühr, B.: Dome growth and coulée spreading controlled by surface morphology, as determined by pixel offsets in photographs of the 2006 Merapi eruption, *J. Volcanol. Geotherm. Res.*, 261, 121–129, <https://doi.org/10.1016/j.jvolgeores.2013.02.004>, 2013.
- Wang, D., Shao, Q., and Yue, H.: Surveying Wild Animals from Satellites, Manned Aircraft and Unmanned Aerial Systems (UASs): A Review, *Remote Sensing*, 11, 1308, <https://doi.org/10.3390/rs11111308>, 2019.
- 730 Westfeld, P., Mader, D., and Maas, H.-G.: Generation of TIR-attributed 3D point clouds from UAV-based thermal imagery, *Photogrammetrie Fernerkundung Geoinformation*, 2015, 381–393, <https://dx.doi.org/10.1127/1432-8364/2015/0274>, 2015.
- Westoby, M. J., Brasington, J., Glasser, N. F., Hambrey, M. J., and Reynolds, J. M.: “Structure-from-Motion” photogrammetry: a low-cost, effective tool for geoscience applications, *Geomorphology*, 179, 300–314. <https://doi.org/10.1016/j.geomorph.2012.08.021>, 2012.



- 735 Yajima, R., Nagatani, K, and Yoshida, K.: Development and field testing of UAV-based sampling devices for obtaining volcanic products," 2014 IEEE International Symposium on Safety, Security, and Rescue Robotics, 1-5, <https://doi.org/10.1109/SSRR.2014.7017680>, 2014.

740